J. Cosmet. Sci., **60,** 547–585 (September/October 2009)

Papers Presented at the Annual Scientific Seminar of the Society of Cosmetic Chemists

June 4–5, 2009
Chicago Hilton
Chicago, Illinois

THE INFLUENCE OF SENSORY PERCEPTION: CONSUMER PERCEPTIONS OF LIKING AND PERFORMANCE

Gail Vance Civille

Sensory Spectrum, Inc.

The sensory properties of personal care products (hair care, skin care, nail care, fragrances and cosmetics) influence the consumer's perceptions, such as, liking, perceived benefits, efficacy and performance. In addition, sensory properties are tied to key consumer attributes such as, creamy, premium, luxury, rich and clean.

Product Understanding

Trained expert descriptive analysis panels with hundreds of hours of training and experience are standard protocols, references, and attribute definitions to create an ***analytical*** sensory tool that documents the fragrance, appearance, and tactile feel of products, including those designed for anti-aging effects. The descriptive analysis data can define the sensory properties of products in a category and can define similarities and differences across a company's product line, it's competitors and selected bench prototypes. When these data are mapped, category appraisal and/or benchmarking the entire product space yields rich insights into the category and the future product possibilities or white space. The product developer can see the product comparisons and the scope of the product category appraisal which enables development of new products that deliver specific sensory signals. The panel can access the new prototypes to confirm that the desired sensory properties are perceivable in the select prototypes. The program is calibrated and highly monitored; see the attribute lists below.

Lotion Attributes	**Skinfeel Attributes**			**Fragrance** Major Categories
Appearance	**Rubout**	**Immediate Afterfeel**	**20-minute Afterfeel**	**Total Impact**
Integrity of shape (immediate)	Wetness	Gloss	Gloss	Floral
Integrity of shape (10s)	Spreadability	Stickiness	Stickiness	Fruity
Gloss	Thickness	Slipperiness	Slipperiness	Citrus
	Oily	Thickness of residue	Thickness of residue	Green
Pick-Up	Waxy	Amount of residue	Amount of residue	Animal / Leather
Firmness	Greasy	Oil	Oil	Herbaceous
Stickiness	# rubs to absorbency	Wax	Wax	Ozone / Marine
Cohesiveness		Grease	Grease	Base
Peaking		Silicone	Silicone	

Detailed skin product profiles are shown below.

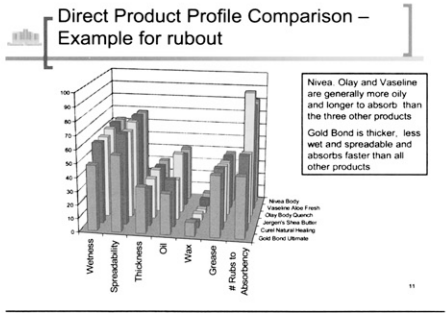

Consumer Understanding

Uncovering consumer unmet needs requires creative and classic tools. Opportunities exist in deep dive qualitative research to discover consumer language, behavior preferences, and needs. These insights stimulate both product and market ideas that R&D and Marketing can use to begin developing concepts and products. Confirmation of success with qualitative consumer research need not be expensive and onerous if the early work has laid the foundation. A community narrative panel [SCAN] can provide fast and rich information about products or concepts. One example

Linking Consumer & Product Understanding

The sensory attributes, provided by the descriptive panel documents the perceived properties of the products and prototypes. The consumer provides responses, such as liking, efficacies, delivering benefits, to the same set of products. Sophisticated qualitative research and sophisticated statistics with quantitative research allow the sensory analyst to discover which fragrance, tactile, appearance or package attributes are aligned with the anti-aging claim or concept.

Sensory panels linked to consumer studies yield rich information and insights into the key drivers of perceived anti-aging performance. Product attributes, fragrance, color, tactile feel, feel of the skin or hair, can reinforce the anti-aging concept.

Creative and classic sensory methods are crucial tools in the discovery of both product design and marketing strategy. Linking product understanding and consumer understanding yields a complete truth about what the consumer wants and how to design the sensory properties to deliver.

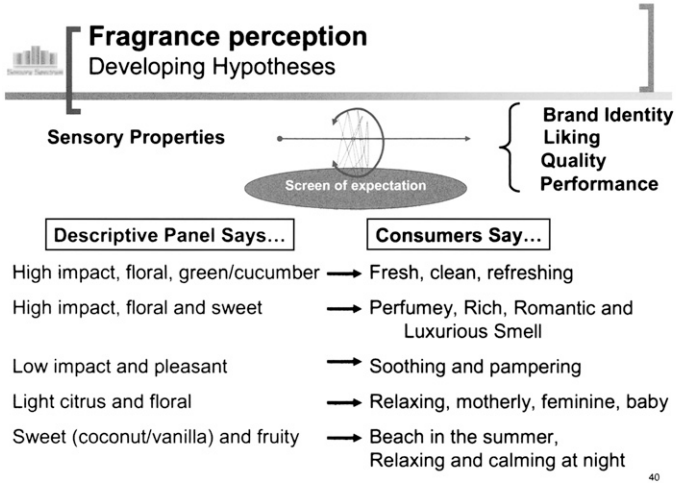

PHYTOCHEMICAL FERMENTATION: A NATURAL WAY TO FUSE PLANT CHEMISTRY AND MICROBIOLOGY TO POTENTIATE SKIN CARE ACTIVITY

Smitha Rao, Judith Bernabe, James V. Gruber, Ph.D., Lisa Bouldin and Maria Dominquez

Arch Personal Care Products, L.P., 70 Tyler Place, South Plainfield, NJ 07080

Introduction

Topical application of botanical extracts has been and continues to be a very actively growing area of ingredient development. Furthermore, topical application of yeast fermentation extracts has shown a significant amount of benefits for many years.[1] Several novel phytochemicals isolated from plants exhibit key functional aspects critical for ameliorating cellular ageing. Current personal care products employ topical applications of the phytochemical to benefit skin's function. We have explored the benefit of fermenting these small molecules by fungi specifically belonging to the genus *Saccharomycetaceae*. Much the way fermentation of grapes can enhance their benefits through wine production, it might be anticipated that the fermentation of unique phytochemicals such as resveratrol, can synergistically potentiate the benefits of both the yeast and the botanical phytochemical. The objective of our work was to evaluate if there was substantial evidence that the metabolic actives obtained from the 'yeast/resveratrol ferment extract' offers distinct advantages to extend the functionality of skin cells that are otherwise unavailable by topical application with unfermented actives.

Methodology

Pichia pastoris was selected as the micro-organism for fermentation of resveratrol; to examine the influence of exposing purified resveratrol on actively growing yeast cultures. Fermentation process was conducted as described.[2.] After optimization of treatment via shake flask trials, the process was scaled up to 2L and 15L fermentation stages (2L New Brunswick Scientific, Edison NJ and 15L Applikon Biotechnology Foster City CA).[2]

LC-MS ANALYSIS OF RESVERATROL

The objective of this analysis was to determine levels of resveratrol in the samples by liquid chromatography-electrospray ionization mass spectrometry (LC-ESI-MS). Samples were taken during various stages of fermentation, separated using a reversed-phase C18 column and analyzed by LC-ESI-MS in the negative ion mode using selective ion monitoring.[3]

IN VITRO ANALYSIS

The testing system used for this assay was the MatTek® full thickness skin tissue model. For this study the tissues were treated topically with test materials for 24 hours. At the end of the treatment period, the tissues were homogenized for analyses of the protein markers using ELISA technique (COX1and COL4A1).[4]

Results

The analysis of resveratrol indicates that the concentration in the final product is below the limit of detection (<1μg/mL) at the end of the fermentation. Based on the results, resveratrol is completely metabolized by the yeast during fermentation (Figure 1).

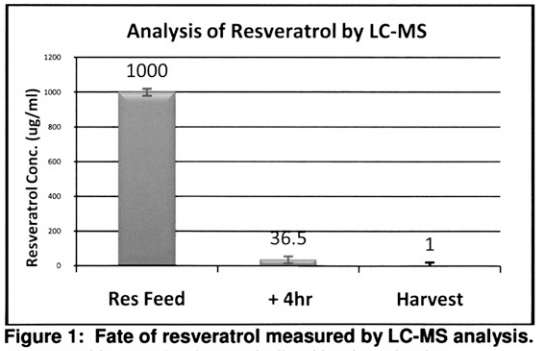

Figure 1: Fate of resveratrol measured by LC-MS analysis. The harvest sample indicates that the resveratrol is completely metabolized by the microbe.

The principle findings from the *in vitro* studies suggest that the application of yeast/resveratrol ferment extract consisting of the metabolized actives of resveratrol impacts various anti-inflammatory markers like COX1; augments extracellular matrix of the skin by promoting the synthesis of Type IV Collagen (Table 1). This activity was not demonstrated by the topical application of resveratrol on the tissue. *In vivo* test results support the *in vitro* studies delivering strong anti-inflammatory and anti-wrinkle benefits.

Table 1: Summary of results obtained from the *in vitro* studies. ⇑ indicates increase in activity, ⇓ indicates decrease in activity and (-) indicates no significant result.

Function	Bio-Marker	Pichia/Resveratrol Treatment	Resveratrol Treatment
Extra-cellular Matrix	COL4A1	⇑	-
Inflammation	COX1	⇓	-

Conclusion

We have successfully developed a method of fermenting yeast which influenced by positive stress originating from small molecules derived from plants. Our efforts focused on 'resveratrol' as the small molecule inducing positive stress on yeast. Also, we have successfully demonstrated the complete utilization of resveratrol by the yeast and bio-conversion of the phytochemical into metabolized actives.

REFERENCES

1. Kaplan, J. Z. "Acceleration of wound healing by a live yeast cell derivative", Arch Surg. 1984 119, 1005-1008.
2. Nagaraj S, Gruber JV, Brooks G (August 2007). The effects of resveratrol stress during yeast fermentation. Society of Industrial Microbiology –Poster #P52
3. Gorg A, Obermaier C, Boguth G, Harder A, Scheibe B, Wildgruber R, Weiss W (2000) The current state of two-dimensional electrophoresis with immobilized pH gradients. Electrophoresis 21: 1037–1053
4. Szewczuk LM, Forti L, Lucia AS and Penning TM. (2004) Resveratrol is a peroxidase- mediated inactivator of COX-1 but not COX-2. JBioChem279:21 22727-22737

A NOVEL HIGH PERFORMANCE WRINKLE CORRECTOR WITH ANTI-"INFLAMM-AGING" PROPERTIES

Carla Perez[2], Sandy Dumont[1], Ph.D., Laetitia Cattuzzato[1], Gerard Trouve[1], Ph.D., Nathalie Chevrot[3] and Corinne Stolz[3]

[1]SEPPIC, Laboratoires de recherché, 127 chemin de la Poudrerie, BP228, 81105 Castres cedex 05
[2]SEPPIC, Inc., 30 Two Bridges Road, Suite 210, Fairfield, NJ 07004
[3]SEPPIC, Tour Kupka C, 7 Bd F. Kupka, 92039 Paris La Defense Cedex, France

Introduction

Ageing is a multi-parametric and cumulative process, resulting from both chronological (or genetic) and external events [1]. Moreover, an ageing-associated hyper-inflammatory state can be observed and is sometimes referred as "inflamm-aging" [2;3]. It is characterised by an increase in the production of pro-inflammatory cytokines, particularly interleukin (IL)-6, and is enhanced by UV irradiation [2;3;4;5;6]. As a result, the increased production of matrix metalloproteases (MMPs) contributes to extracellular matrix (ECM) and dermo-epidermal junction (DEJ) degradation. Dermatopontin (DPT) is a small acid protein which is involved in collagen fibrillogenesis and promotes activity of Transforming-Growth Factor (TGF)-β1 [7]. This multifunctional growth factor promotes fibroblast growth, ECM production and expression of tenascin C (TNC), which is involved in tissue remodelling [8]. During ageing, the observed decrease in TGF-β1 fibroblast stimulation accentuates the collagen/MMP/TIMP (Tissue Inhibitors of MMPs) balance impair [9;10;11;12]. All together, these modifications lead to dermis atrophy. Fibroblast migration and interactions with ECM are impaired, leading to a loss of ECM network contraction and, thus, of firmness. In addition, in aged skins, a decrease in the size and/or the number of dermal vessels as well as in skin vascularity is observed [13;14], leading to a reduced nutritional support, pallor and loss of skin radiance [13;14;15]. In conclusion, when aging, skin becomes more inflamed, stressed, less protected, less nourished, and becomes withered, fragile, dull, tired and wrinkled. The aim of this study was to demonstrate Palmitoyl Glycine (PG) ability to rejuvenate cell/tissue phenotype through inflammation reduction, improvement of ECM production/organization, and radiance boosting; and thus to confirm the actions of PG in slowing the aging mechanism.

Materials and Methods

Analysis of differential gene expression

Analysis of differential gene expression was performed by BIO*alternatives* (Gençay, France). A pool of normal human fibroblasts (average age: 30y) was serially cultured for 8 or 17 passages, thus leading from young to senescent (ageing) fibroblasts, respectively. Fibroblasts were treated or not by PG (0.001%; Seppic) and incubated for 96h. RNA extraction, cDNA arrays and quantitative-polymerase chain reaction (q-PCR) confirmation experiments were performed by BIO*alternatives*. The array contained 149 duplicate fibroblast-associated cDNAs and housekeeping markers. The procedure used was approximatively the same as that previously described by Bernard *et al.* [16].

Fibroblast culture and photo-ageing model

Normal human dermal fibroblasts (Lonza) were seeded in 24-microwell culture plates and cultivated for 5 days at 37°C, 5% CO_2. On day 5, cells were incubated or not with PG (0.001% (w/v)) for 72 hours. Cells were then irradiated or not with 10 J/cm^2 UVA rays and further cultivated in the presence or not of PG for 24 hours. After the 96h incubation period, cell supernatents were removed and stored at –80°C. Cells were rinced and lysed by ultrasounds. Extracellular TIMP-2 (TIMP-2, Human, Biotrak ELISA System, GE healthcare) and intracellular type I procollagen (Procollagen Type I C-Peptide EIA Kit Manual, Takara) contents were quantified with ELISA experiments. Total protein contents were quantified using the Coomassie blue method, as previously described [17]. Results were expressed in ng/mL (TIMP-2, procollagen) or in mg/mL (proteins).

Tubular formation assay

Normal Human Umbilical Vein Endothelial Cells (HUVEC; Lonza) were cultured at 37°C, 5% CO_2 in EBM-2 (Lonza) supplemented with 1% FBS on Matrigel™ (BD Biosciences)-coated 96-microwell plates. After a 16-hour incubation period in the presence or not of the diluted tested products (10ng/mL VEGF, Sigma-Aldrich or 0.00005% (w/v) PG), images of each condition were captured and the number of capillary nodes was manually counted (an increase in the number of capillary nodes reflecting a better organization of microvascular network). A fluorescent labelling with 1mM Calcein AM (Sigma-Aldrich) was then performed in order to ensure viability of the pseudo-tubular structures. The neovascularisation-associated activity was then calculated.

Skin radiance assay

Human skin explants were placed in 6-well plates and cultivated in Skin long term culture medium (Biopredic) at 32°C, 5% CO_2. After one "recovery" night, formulations were topically applied (2mg/cm^2). Topical applications and medium renewal were repeated every two days or three days until day 14. L (luminosity) and a* (erythema) parameters were measured on skin explants on day 0 and day 14 with a Chromameter® CR-400 (Konica Minolta). Analysis was performed in quadriplicates. The variations $\Delta(D_{14}-D_0)$ of L and a* parameters were calculated for each explant. Skin radiance promoting and anti-erythematic efficacies were then calculated.

Data analysis and statistical analysis

All experiments were performed in triplicates (except for specified protocols). For each group, the mean and the standard deviation were calculated, reported to the control group and expressed as variation percentages. Statistical significance was assessed using a two-tailed, paired Student's test. In some cases, a restoration or photoprotection percentage was calculated.

Results

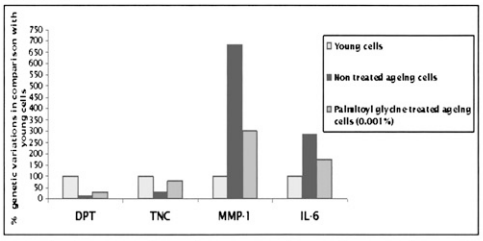

Figure 1 : Quantitative relative expression (RE) of genes encoding DPT, TNC, MMP-1 and IL-6 in young fibroblasts and either LAA-treated or not ageing fibroblasts. Results are expressed in variation percentages relative to the RE observed on non ageing cells (qPCR experiments).

Palmitoyl glycine partially restores the genetic profile of ageing normal human dermal fibroblasts

Results obtained with the cDNA minichips study showed that genetic variations induced by the ageing process of normal human fibroblasts were restored by a PG treatment (data not shown). A few variations were then confirmed by performing qPCR experiments, this method being more sensitive and quantitative. PG showed a restoration effect on the ageing-induced increase in MMP-1 and IL-6 gene expression level, respectively of 66% and 60% (Figure 1). It also showed a restoration effect on the ageing-induced decrease in DPT and TNC gene expression level, respectively of 17.5% and 74%.

Palmitoyl glycine promotes and exerts a photo-protection on type I collagen and TIMP-2 productions

In irradiated (10 J/cm^2 UVA) or not irradiated fibroblast cultures, Palmitoyl Glycine tested at 0.001% induced a significant increase in type I collagen (respectively +13.5%, $p<0.05$ and +21%, $p<0.05$) and TIMP-2 productions (both of +29%). The mean photo-protective effects were thus of 136% and 222%, respectively for type I collagen and TIMP-2 (data not shown).

Palmitoyl glycine promotes the formation of new blood vessels in an in vitro 3D-model

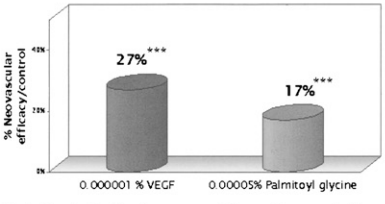

As expected, the positive reference molecule, VEGF, tested at 10ng/mL, induced a statistical significant increase in the number of capillary nodes, *i.e.* +27% ($p<0.001$; Figures 2 and 3). The negative reference molecule, fumagillin, tested at 30µg/mL, induced a statistical significant decrease in the number of capillary nodes, *i.e.* -45% (data not shown). PG tested at 0.00005% induced a statistical significant increase in the capillary nodes, *i.e.* +18% ($p<0.001$; Figure 2).

Figure 2: Neovascularisation-promoting activities: comparison of Palmitoyl glycine with VEGF. *: statically significant results (Student T test, $p<0.001$)**

Palmitoyl glycine improves skin radiance of skin explants

Palmitoyl Glycine formulated at 1% and topically applied on the surface of skin explants induced an almost statically significant increase in the luminosity-associated chromametric parameter L of +5%, after a 14 day-treatment ($0.05<p<0.1$; data not shown). It also induced a decrease in the erythema-associated chromametric parameter a* of 24% after a 14 day-treatment ($p<0.05$; data not shown).

Discussion and Conclusion

Palmitoyl glycine (PG) showed a great ability to restore the youth-associated genetic profile of normal human fibroblasts. Indeed, it prevented the ageing-induced gene expression variations observed on the pro-inflammatory cytokine IL-6, the ECM degrading enzyme MMP-1, the collagen fibre organization-promoting factor DPT and the ECM remodelling-related protein TNC. Given that IL-6 favours the aging-induced impairment of the collagen/MMP/TIMP balance [18], we investigated whether PG could also act on type I collagen and TIMP-2 productions. As expected, PG was able to improve both productions from fibroblast cultures and to exert a photo-protective effect. These results illustrate the fact that PG can act on different levels and make it appear as an interesting candidate to breakdown the vicious circle of "inflamm-aging" [2]. Another interesting feature of PG is its ability to improve the microvascular network by promoting new vessels formation and tubular organization. These *in vitro* observations were confirmed by *ex vivo* investigations since the repeated topical applications of a PG-containing formula to the surface of skin explants led to an improvement in the luminosity-associated chromametric parameter L and thus, in skin radiance. Conversely, it induced a decrease in the erythema-associated chromametric parameter a*, which confirms its anti-inflammation activity. In conclusion, PG enables a regulation or a restoration effect on main ageing-associated disorders. Indeed, it can not only act on tissue architecture and extracellular matrix protection but also on inflammation and skin radiance. Finally, a clinical trial performed on Caucasian women (1% PG-containing formulation, 42d-treatment on crow feet) confirmed PG wrinkle corrector efficacy, which was superior to that of a market reference ingredient (formulated at 3%).

References

[1] Fisher GJ, Kang S, Varani J, Bata-Csorgo Z, Wan Y, Datta S, Voorhees JJ. *Arch Dermatol.* **138**, 1462-70 (2002).
[2] Kovacs EJ. *Exp Gerontol.* **40**, 549-55. (2005)
[3] Bennett MF, Robinson MK, Baron ED, Cooper KD. *J Investig Dermatol Symp Proc.* **13**, 15-9. (2008).
[4] Bickers DR, Athar M. *J Invest Dermatol.* **126**, 2565-75. (2006).
[5] Walston J, Xue Q, Semba RD, Ferrucci L, Cappola AR, Ricks M, Guralnik J, Fried LP. *Am J Epidemiol.* **163**, 18-26. (2006).
[6] Omoigui S. *Immun Ageing* **4**, 1. (2007).
[7] Okamoto O, Fujiwara S. *Connec. Tiss. Res.* **47**, 177-89. (2006).
[8] Jinnin M, Ihn H, Asano Y, Yamane K, Trojanowska M, Tamaki K. *Oncogene.* **4**, 1656-67. (2004).
[9] Zeng G, McCue HM, Mastrangelo L, Millis AJ. *Exp. Cell. Res.* **228**, 271-6. (1996).
[10] Ashcroft GS, Herrick SE, Tarnuzzer RW, Horan MA, Schultz GS, Ferguson MW. *J Pathol.* **183**, 169-76 (1997).
[11] Chung JH, Seo JY, Choi HR, Lee MK, Youn CS, Rhie G, Cho KH, Kim KH, Park KC, Eun HC. *J Invest Dermatol.* **117**, 1218-24 (2001).
[12] Rittié L, Fisher GJ. *Ageing Res Rev.* **1**, 705-20. (2002).
[13] Chang E, Yang J, Nagavarapu U, Herron GS. *J Invest Dermatol.* **118**, 752-8 (2002).
[14] Chung JH, Yano K, Lee MK, Youn CS, Seo JY, Kim KH, Cho KH, Eun HC, Detmar M. *Arch Dermatol.* **138**, 1437-42 (2002).
[15] Toyoda M, Nakamura M, Luo Y, Morohashi M. *J Dermatol Sci.* **27**, 32-41. (2001).
[16] Bernard FX, Pedretti N, Rosdy M, Deguercy A. *Exp Dermatol.* **11**, 59-74 (2002).
[17] Bradford MM. *Anal Biochem.* **7**, 248-54 (1976).
[18] Wlaschek M, Heinen G, Poswig A, Schwarz A, Krieg T, Scharffetter-Kochanek K. *Photochem Photobiol.* **59**, 550-6 (1994).

BIOFLAVONOIDS: BENEFITS FOR SKIN AND FORMULATING "GREEN"

Howard Epstein[1], Frank Pfluecker[2], Ph.D., Corinna Wirth[2], Ph.D., Ruediger Graf[2], Ph.D., Maria Prenzel[2], Bettina Magsaam[2] and Michelle Quinn

[1]EMD Chemicals, Inc., Gibbstown, NJ
[2]Merck KGaA, Darmstadt, Germany

INTRODUCTION:

Nature's solutions have been used to combat health problems since ancient times. Over 3,000 years ago the use of medicinal plants to treat skin diseases was documented in the papyrus Ebers . The traditional description for use of medicinal plants is generally not linked to topical application. The interrelationship of seemingly different health problems is not always obvious. For example a plant used to treat diabetes may be useful to help prevent wrinkles or perhaps to reduce inflammation, acne and itching. The ability to identify new cosmetic uses for botanicals is enhanced when science is able to advance beyond anecdotal information to elucidation of the mechanism of activity. Once the mechanism of activity is elucidated there is an opportunity to decide the most appropriate form for delivery of the plant's "active(s)." Is a standardized or enriched extract, a purified compound directly isolated from plants, a modified isolated natural compound more desirable? In the example presented, the bioflavonoid Tiliroside found in a variety of medicinal plants including tilia, malva appears to have the reported activity described below as a single compound. Tiliroside is found in the hairy protrusions and young leaves of plants growing in tropical regions of the world. Tiliroside protects plants from ultraviolet-induced and environmental stress.
The aim of this study was to demonstrate that the bioflavonoid responsible for protecting the plant from environmental stress can also provide benefits for people. *In vitro* and *in vivo* methods were used to generate the data. Two bioflavonoids were evaluated , Tiliroside and isoquercetin which was evaluated for antoxidant activity using a variety of methods.

METHODOLOGY:

Anti-inflammation: Twenty healthy female volunteers with dry skin were evaluated for their response to UV (ultraviolet)-induced erythema and change in capillary blood flow. Inflammation was stimulated by UV irradiation to the inner forearms of the volunteers (one MED, SOL3 Honle, Munich, Germany). Resulting erythema was documented using two measuring devices during a three day period. Color measurements were recorded with a Minolta Chromameter CR 300 using the reddening index a-value. A Laser-Doppler Flowmeter was used to determine capillary blood flow. The erythema threshold was determined for each test subject individually using different light intensities. The development of erythema was evaluated after application of a negative control (untreated) area, an oil-in-water emulsion and a test oil-in-water emulsion containing 0.1% Tiliroside. A 1% hydrocortisone cream was used as a positive control. One test area was untreated (empty field) and was not irradiated or treated. The combined measurements enable the documentation of a possible anti-inflammatory effect. The appearance of erythema is evaluated after application of each test material immediately after application, then 6, 24 and 48 hours afterwards. Each site was compared to the untreated reference and the site treated with 1% hydrocortisone. Data was evaluated statistically using the area under the curve. All measured data for each treatment group was compared in pairs by means of the Wilcoxon Sign Rank test. For all tests a p-value$\leq$ 0.05 was fixed as statistically relevant.
Antioxidant Activity: Isoquercetin a derivative of rutin was evaluated for antioxidant potential using various *in vitro* methodologies as follows; the Rancimate assay determines the relative molar protection factor of stabilized soy bean oil compared to non-stabilized soy bean oil. A lipid assay was used to assess the potential to inhibit peroxidation relative to α-tocopherol, the test radical used is 2,2'-azobis(2-aminepropane). The TEAC (Trolox equivalent antioxidant capacity) assay compares the ability of an antioxidant to scavenge radicals to Trolox, a synthetic analogue of α-tocopherol. A DPPH (α,α-diphenol-β-picrylhydrazyl radical) assay measures the ability to reduce the stable radical DPPH, the lower the amount requires the more efficient the antioxidant. Xanthine oxidase determines the amount of antioxidant required to inhibit enzymatic 0_2^- generation. An NBT (nitroblue tetrazolium) assay was run to determine the capacity to scavenge non-enzymatically generated O_2^-, in this assay superoxide anion radicals reduced the substance to NBT.

RESULTS:
Anti-inflammation: The untreated control showed a relatively strong increase in skin reddening 6 hours post-irradiation with a slight increase at 24 hours. After 48 hours the reddening slightly subsided. The placebo showed a very weak efficacy with an increase of reddening slightly below the untreated test field. The test site treated with the formulation containing 0.1% Tiliroside showed a distinct effect regarding reduced reddening compared to the untreated site figure 1). The site treated with 1.0% hydrocortisone showed the most reduced reddening. Measurement of capillary blood flow (figure 2) increased in the untreated control to a maximum 24 hours after irradiation. The untreated control and the placebo emulsion showed the lowest efficacy. The emulsion with 0,1% Tiliroside showed diminished capillary blood flow after 6, 24 and 48 hours post-UV exposure compared to the untreated control and placebo, the highest efficacy was achieved by 1% hydrocortisone formula (positive control). No significant changes were observed in the empty field which was untreated and not irradiated.
Antioxidant activity: Results of the rancimate assay varied with the method used (figure 3). The TEAC method indicated isoquercetin is comparable to butylated hydroxytolune (BHT), a known antioxidant, in the xanthine oxidase method isoquercetin tested to be superior to α-Tocopherol, Isoquercetin was more effective than BHT using the DPPH assay.

CONCLUSIONS:
Bioflavonoids can provide anti-aging benefits as shown by the described studies. Erythema reduction and improvement in capillary blood flow which are an indication of an inflammatory process were both shown to be significantly improved compared to the control and a placebo. The measured antioxidant potential of a substance may vary with the different test methods and test parameters used to measure the activity. For this reason a variety of antioxidant assays are suitable to evaluate the ability of a material to protect from free radical radicals. Good study design is essential to duplicate results which are critically important when investigating flavonoids. This information helps to validate published literature supporting nourishing, healing and anti-aging effects of the flavonoids.

Figure 1: Redness (Minolta a-Value)

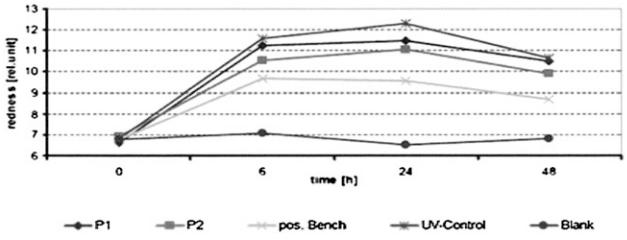

P1 Placebo, P2 0,1% Tiliroside Sorbitol, pos.Bench 1% Hydrocortisone UV-Control=UV-irradiation without treatment
Blank=no irradiation, no treatment, n=20

Figure 2: Capillary Flow

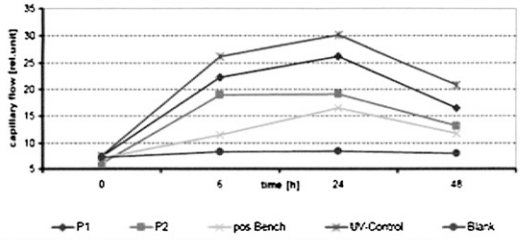

P1 Placebo, P2 0,1% Tiliroside Sorbitol, pos.Bench 1% Hydrocortisone UV-Control=UV-irradiation without treatment
Blank=no irradiation, no treatment, n=20

Figure 3; Isoquercetin

Protection from free radicals

	Rancimate Merck relative molar prot.factor	Rancimate von Gadow Induction time hours	Lipid assay Merck relative antiox. Efficiency	TEAC assay Merck Trolox equivalent mg/L	Xanthine oxidase Masuoka IC_{50} of O_2^- generation
Isoquercetin	1,23	4,17	0,57	0,54	41,00
BHT*	1,72	4,08	0,85	0,50	
α- Tocopherol	1,25	3,16	1,00		240,00
Trolox					

	DPPH assay Merck EC_{50} in mg antioxidant	DPPH assay von Gadow % inhibition	DPPH assay Joubert % inhibition	DPPH consumption Masuoka no. molecules per antioxidant	NBT reduction Joubert % inhibition of O_2^- generation
Isoquercetin	105,00	91,99	86,59	6,54	66,67
BHT*	86,00	45,58			
α- Tocopherol		75,10		2,65	
Trolox			58,10		5,31

*BHT = butylated hydroxytoluene best 2nd weakest antioxidant

13C-NMR ANALYTICAL STUDY TO DETERMINE FREE FORMALDEHYDE AVAILABILITY ON TWO FORMALDEHYDE DONORS: IMIDAZOLIDINYL UREA AND DIAZOLIDINYL UREA

Michael Tallon, Ph.D., John J. Merianos, Ph.D. and Sangeetha Subramanian

International Specialty Products, 1361 Alps Road, Wayne, NJ 07470

Formaldehyde donors such as imidazolidinyl urea (IU) and diazolidinyl urea (DU) are very effective preservatives that have been used in consumer products for several decades. It is well known that the analysis of free anhydrous formaldehyde (FA) in the presence of formaldehyde donors can yield inaccurate results[i]. An equilibrium exists in an aqueous environment, where most of the formaldehyde is hydrated and exists predominantly in the form of methylene glycol (99.96%). Only a very small fraction is available as free formaldehyde gas (0.04%) [ii,iii]. Methylene glycol has reduced reactivity and volatility as compared to free formaldehyde.

Table I: Aqueous solution equilibrium for formaldehyde in water[ii]:

$$HCHO\ (g)\ \text{(Free Formaldehyde)}\ (0.04\%) + H_2O \longleftrightarrow HOCH_2OH\ \text{(Methylene Glycol)}\ (99.96\%)$$

$$K\ [H_2O]\ 25°C = 2 \times 10^3$$

Almost all of the known analytical methods and many of the analytical reagents used for determination of free formaldehyde are destructive to formaldehyde donor molecules that are present in equilibrium as isomeric species[iv, v]. Likewise, testing conditions may not reflect actual pH and / or concentration in the product to which the free FA levels reported are being extrapolated. The total formaldehyde sometimes reported includes not only the free formaldehyde but also methylene glycol and the bound formaldehyde (N-methylol functionality). For example, the wet chemistry method (acetylacetone) is commonly practiced - Both the European (EEC) and the Japanese methods are based on using acetylacetone as a derivatizing reagent but differ in the temperature of the derivatization and the duration of the reaction that can detect down to 1 ppm. Other wet chemistry methods include using 1, 3-dihydroxy-naphathalen (DHN) as a derivitizing agent or using reagents such as chromotropic acid (CA) and hydrogen peroxide. Table II compares results from different methods for FA determination vs. theoretical weight % of FA. Hence, the values reported in Table II is the total titratable formaldehyde, and not exclusively free formaldehyde per se.

TABLE II – Comparison of several analytical methods for FA determinations

Product	Theoretical % FA in product	EEC	Japan	DHN	CA	H_2O_2
Formalin	37	100	100	100	100	100
IU	23.2	32.3 - 40.5	27.2 - 39.4	32.8	55.2	40.7
DU	43.3	39.2 – 47.6	34.2 – 40.4	49.2	67.9	49.4

The objective of this study was to use a non-invasive, non-destructive analytical method, 13C – NMR, to analyze for the level of free FA available on two formaldehyde donor preservatives: IU and DU. This technique is currently the only accurate method for formaldehyde analysis in complex formulation matrices containing UV chromophores. It requires no sample preparation, and is not restricted to any given pH or concentration, thus providing results of an un-altered sample and a more realistic level of actual free FA in the product. This technique determines the level of methylene glycol in the sample from which the free formaldehyde level is then calculated according to the following equation:

$$\text{(a). Free FA (ppm)} = \frac{\text{Methylene glycol (ppm)} \times 0.04\%}{99.96\%}$$

The 13C-NMR spectra for IU and DU in water at pH 7.5 are illustrated in Figures 1 and 2, respectively. Methylene glycol is easily detected at 85 ppm while the bound formaldehyde of the N-methylol carbons spans 70 – 40 ppm. The multiplicity of the N-methylol carbons confirms the presence of a complex equilibrium mixture of isomers spanning the available nitrogen atoms within the molecule as depicted on each spectrum.

Figure 1

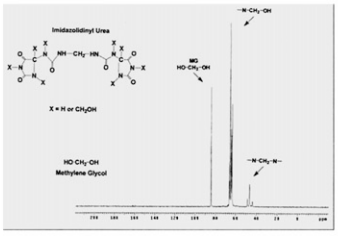

Figure 2

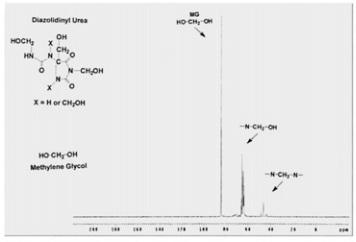

The quantitative 13C-NMR results for IU and DU in water are summarized in Table III. For IU, most of the total formaldehyde is actually bound to the molecule (85%) as evidenced by the integral ratios to methylene glycol. This differs significantly from the results obtained by wet chemistry and chromatographic methods which indicate the presence of 40 – 55 % free FA. A similar result is observed for DU. Therefore, the EEC and the Japanese methods significantly underestimate the level of methylene glycol present.

Table III: Free FA concentration using acetylacetone method vs. 13C-NMR (recommended use level, pH 7.5, 25 °C)

Product in water	Use level	Total FA (acetylacetone)	ppm total FA by acetylacetone[1] (calculation)	ppm methylene glycol by 13C –NMR	ppm free FA (calculation)
IU	0.6%	9.39%	564	88	0.035
DU	0.3%	20.6%	618	387	0.154

Note [1]. Calculation according to equation (a).

According to the 13C-NMR analysis, IU contains less than 0.04 ppm and DU less than 0.2 ppm free FA in water. This shows that the actual level of free formaldehyde present in the formaldehyde donors studied in aqueous formulations is three orders of magnitude lower as compared to other wet chemical 'batch' methods. This is because a significant portion (40 – 85%) of the total FA is still bound to the FA donor and the remaining moiety is methylene glycol. These results clearly reflect the superiority of the spectroscopic method over other available methods which typically tend to overestimate the amount of free FA present. The 13C-NMR method is non-invasive, non-destructive and measures free formaldehyde without affecting the equilibrium of formaldehyde donor type preservatives.

---

[i] Emeis, D., Anker, W. and Wittern K-P. *" Quantitative 13C- NMR Spectroscopic Studies on the Equilibrium of Formaldehyde with Its Releasing Cosmetic Preservatives*" Analytical Chemistry, **79.** 2096-2100 (*2007*)

[ii] Walker, J.F. Formaldehyde 3rd. Edition. 59-61; Table 14 (*1964*)

[iii] Kirk-Othmer Ency. of Chemical Technology. 929-951. Chapter 11 (*1994*)

[iv] Rossmoore, H.W. and Sondossi, M. "*Applications and Mode of Action for Formaldehyde Condensate Biocides*". Advances in Applied Microbiology, **33.** 223-277 (*1998*)

[v] Merianos, J.J. Sondosi M. Wachocki, B. A. and Rossmoore H. W. "*Factors Involved in Mode of Action of Imidazolidinyl Urea and Urea Biocides*". Preservatech Conference Proceedings May 27. 29 - 38 (*1998*)

TECHNIQUES OF DEFORMULATION (REVERSE EMGINEERING)

Paul Winter, Ph.D.

Chemir Analytical Services, Maryland Heights, MO

Overview

Deformulation or reverse engineering of a personal care product is described as the identification and quantitation of compounds in the product. This is the end result of multiple chemical and physical analysis techniques. It is very important to note that this is the result, but not the goal of the deformulation. The goal of a deformulation is how the results will be used.

The goal of a deformulation is the most important aspect of any project. These goals generally fall into several broad categories. These include deformulation with the goal of a new or reformulated product, reverse engineering of a competitors product, reverse engineering of a product who is marketed by a company but the formulation is not known (third party manufacturing), deformulation for the purpose of label claims, deformulation for the purpose of quality control, and deformulation for legal reasons (label claim, trade secrets, patent infringement). Each of these goals directs the chemical and physical analysis techniques that need to be performed and importantly to what degree that these analysis are performed. For example if the goal of the deformulation is for quality control purposes great attention will be placed upon developing methods that can be repeatedly performed both economically and in a timely manner. This may contrast to a deformulation that is performed for legal reasons in which methods that will both pass a legal challenge in a court of law, but will likely only be performed once. In addition the depth of which a deformulation is performed is also dictated by the goal.

Case Study

The technical aspects of deformulation will be presented in this paper as a case study. This study involves the deformulation of a topical gel, specifically acne treatment gel.

The analytical techniques used in this deformulation were:

High Performance Liquid Chromatography	Quantitation
Liquid Chromatography/ Mass Spectroscopy	Identification and quantitation
Fourier Transform Infrared Spectroscopy	Identification
Nuclear Magnetic Resonance	Identification and Quantitation
Thermogravimentric Analysis	Quantitation
Gas Chromatography Mass Spectroscopy	Identification and Quantitation
Gas Chromatography Flame Ionization Detection	Quantitation
Gel Permiation Chromatography	Quantitation
Karl Fischer	Quantitation
Atomic Emission Spectroscopy	Identification and Quantitation

The approach to this study was to first identify the components or component types that were present in the product. The second step was to perform quantitation of the component. Table 1 lists the identification and concentration of the compounds found in the product.

Table 1

The following table lists the composition of the product:

ANALYTE	QUANTITATION TECHNIQUE	WEIGHT % OF SAMPLE
Active ingredient		1.00 (label claim)
Benzoyl peroxide	HPLC	5.00 (label claim)

Carbomer	HATR	1.51 (8.4% RSD)
Dimethicone	NMR	0.13
Disodium lauryl sulfosuccinate	HPLC	0.08 (4.9% RSD)
EDTA disodium	HPLC	0.08 (9.1% RSD)
Glycerin	GC-FID	3.81 (3.5% RSD)
Silicon dioxide	TGA	0.42 (3.1% RSD)
Methylparaben	HPLC	0.15 (0.6% RSD)
Poloxamer	GPC	0.17 (0.04% RSD)
Purified water	Karl Fischer	87.43 (0.1% RSD)
Sodium hydroxide	AES	0.37 (1.5% RSD)

The volatile components were identified via GC/MS. There were several components not listed in Table 1 that were observed in trace levels. These components were deemed not important, or were found to be by products of the ingredients detected. Although several of the components listed in Table 1 were observed in the GC/MS different techniques were used to quantify, for example HPLC was used to quantify the methylparaben and glycerin.

As expected in most personal care products surfactants and other larger molecular weight compounds were not identified via GC/MS. For these compounds NMR was one technique used for identification. Table 2 shows the results of these analyses.

Table 2 Components Identified in the product via NMR

METHANOL SOLUBLE	HEPTANE SOLUBLE	INSOLUBLE
Disodium lauryl sulfosuccinate	Benzoyl peroxide 5.00% (HPLC)	Carbopol 1.49% (HATR)
EDTA disodium 0.08% (HPLC)	Dimethicone 0.13% (NMR)	Silicon dioxide 0.41% (TGA)
Glycerin 3.81% (GC-FID)	Methylparaben 0.15% (HPLC)	-
Poloxamer 0.17% (GPC)	-	-
Sodium hydroxide 0.37% (AES)	-	-

As observed for the GC/MS analysis, identification was often followed by a different method for quantitation.

LC/MS was used an additional identification tool for non-volatile components. Table 3 lists the results from this analysis.

TABLE 3 Components Identified in the product via the LC/MS Screen

COMPONENT	TECHNIQUE
benzoyl peroxide	HPLC
disodium lauryl sulfosuccinate	LC/MS
EDTA disodium	HPLC
methyl paraben	HPLC

The quantitation was performed via the techniques listed in Table 1.

IMPROVED HPTLC SEPARATION OF LIPIDS AND PHOSPHOLIPDS IN COSMETICS BY USING AUTOMATED MULTIPLE DEVELOPMENT (AMD)

Ingo Schellenberg, Ph.D. and Kathrin Kabrodt, Ph.D.

Anhalt University of Applied Sciences
Institute of Bioanalytical Sciences (IBAS)
Strenzfelder Allee 28, 06406 Bernburg, Germany

Introduction

An increase resolution of thin layer chromatography can be achieved by using Automated Multiple Development (AMD). Using this method the thin layer is developed with a reproducible stepwise elution gradient from polar to unpolar. The aim of our investigations was to show the suitability of HPTLC as a good tool for qualification and quantification of lipids and phospholipids in cosmetics and for determination of major stratum corneum lipids.

It is well known, that ceramides are sphingolipids consisting of sphingoid bases, which are amide-linked to fatty acids. In the stratum corneum (SC), which represents the outer layer of the skin, ceramides play a key role in maintaining the barrier function of skin and in protecting skin against excessive water loss. Various skin diseases such as atopic dermatitis and psoriasis have been reported to be related to impairments in the SC ceramide profiles [1].

The stratum corneum ceramides show a complex structural variability, which poses a challenge for their analysis. Therefore a new HPTLC method with automated multiple development (AMD) was developed that allows a fast separation of the above mentioned substances with an easy gradient.

In comparison to classical TLC procedures and the up to now existing AMD-methods [2,3], our new AMD-HPTLC method is less time and solvent consuming and increases the attractiveness of thin layer chromatography by using AMD.

Materials and Methods

Standard substances with the symbols used are shown in table 1.

table 1: Standard substances

SM	sphingomyeline	**PC**	phosphatidylcholine	**C3S**	sodium cholesteryl-3-sulfate
AP	Ceramide AP	**AS**	Ceramide AS	**NP**	Ceramide NP
MIX	lipid mixture	**NS**	Ceramide NS	**OA**	oleic acid
C	cholesterol	**GT**	glyceryl trioleate	**CO**	cholesteryl oleate
SQ	squalene				

SM, C, CO and Ceramid AS were purchased from Fluka (Taufkirchen, Germany). SQ, PC, GT, C3S and OA were purchased from Sigma-Aldrich (Taufkirchen, Germany). Ceramide NS was provided by Sederma (Le Perray en Yvelines, France) and D,L-Ceramide NP and D,L Ceramide AP were provided by Evonik Industries AG, Germany) Standard lipid mixture consisting of all compounds (concentration from 0.09 to 0.35 mg/ml in methanol : chloroform=1:1, v/v).

Application: 8 mm bands , 5 µl single standard and standard lipid mixture by ATS 4 (CAMAG, Swtizerland); Stationary phase: HPTLC glass plates 20 x 10 cm (silica gel 60 F_{254}, 0.1 mm, Merck), pre-washed twice with chloroform:methanol (2:1; v/v) and activated 30 min at 120 °C in a drying oven; mobile phase: 8 steps gradient based on methanol / chloroform / toluene / n-hexane; development: AMD 2 apparatus (CAMAG); derivatization: using a TLC chromatogram immersion device with a mixture of 10 % cooper sulfate in 8 %phosphoric acid with following drying on a TLC plate heater (CAMAG); detection: TLC Scanner 3 and Reprostar 3 video system (both CAMAG)

Results and Discussion

For optimal separation an 8 steps gradient based on methanol / chloroform / toluene / n-hexane has been developed (for details see picture 1). By using 100 % methanol for the first step all polar substances were completely eluted. Steps two to six separated cholesterol-3-sulfate and the different ceramides. Step seven (100% chloroform) was used for separation of cholesteryl oleate from glyceryl trioleate. In the last step with solvent n-hexane : toluene (95 : 5; v/v) squalen was positioned far away from cholesteryl oleate but under the solvent front.

To focuss oleic acid a chemical preconditioning of HPTLC-plate with 4 molar acetic acid was very important before step six was started.

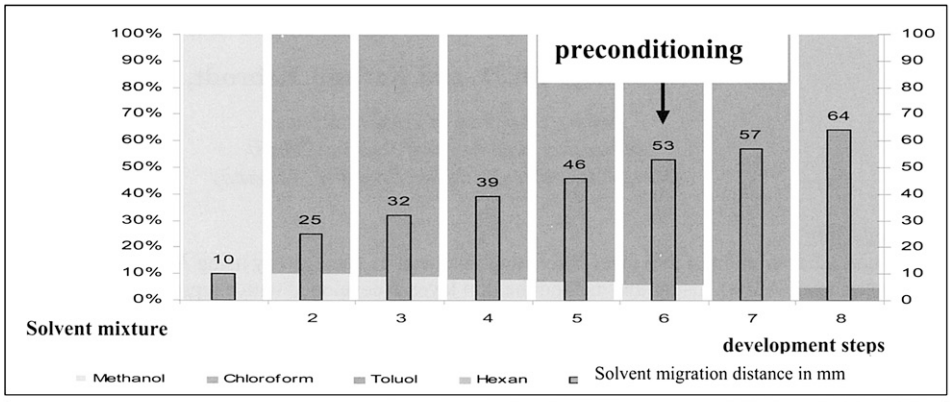

Picture 1: Gradient with 8 steps based on methanol / chloroform / toluene / n-hexane

The densitometric chromatogram (pic.2) shows a successful separation of the above mentioned substances.

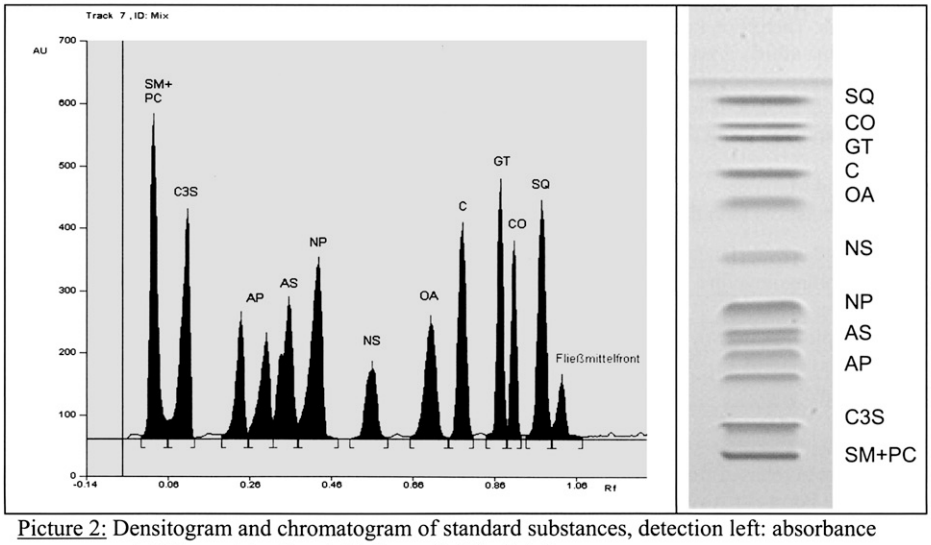

Picture 2: Densitogram and chromatogram of standard substances, detection left: absorbance measurement 600 nm, detection right: image (white light)

CONCLUSION

Besides the excellent separation of the above mentioned substances the 8-step gradient has additional benefits. On the one hand, the total development time is significantly reduced from 6.48 h [2] or 2.30 h [3] to 1.36 h. On the other hand due to the limited number of only 8 steps also the solvent consumption is significantly lower. Additionally to [4] the diastereomers of D,L-ceramide AS has been separated into two bands (pic. 2, right column). The new method also reduces the secondary solvent fronts (accumulation of additives from the solvents) which can interfere with the evaluation.
Additional investigations are required to adopt this method for human sc lipid samples or other samples.

Literature

[1] Motta S., Sesana S., Ghidoni R., Monti M.; *Arch. Dermatol. Res.*, **287,** 691-694. *1995*
[2] Bonté F.; Pinguet P.; Chevalier J.M.; Meybeck A..; *J Chromatogr B* **664**, 311-316. *1995*
[3] Farwanah H., Raith K., Neubert R., Wohlrab J.; *Arch. Dermatol. Res.*, **296,** 514-521. *2005*
[4] .Farwanah H., Neubert R., Zellmer S., Raith K; *J. Chromatography B* **780,** 443-450. *2002*

THICKNESS OF THE LIQUID FILM LEFT BEHIND A MOVING WET WIPE: THEORETICAL AND EXPERIMENTAL STUDY

Gerardo Callegari[1], Ph.D., , A. Baker[2], K. Zwick[3], P. Kaplan[1], A. Neimark* and I. Tyomkin[1]

[1]TRI/Princeton, Princeton, NJ 08540
[2]Kimberly-Clark Corporation, Roswell, GA
[3]Kimberly-Clark Corporation, Neenah, WI
**Department of Chemical Engineering, Rutgers University, Piscataway, NJ*

gcallegari@triprinceton.org

INTRODUCTION

Wetness perception is one of the most important quality assessments for consumers to choose among different wipes. Also, the ability to meter a certain amount of a benefit on a surface (skin, etc) is a key wipe property for developers. Both important properties are intimately related with the thickness of the film left behind after wiping.

EQUATION:

The objective of the present work is to find an equation for the thickness of the liquid film (h_∞) left-behind by a wipe when the liquid is Newtonian, has a viscosity η, and a surface tension γ, and the acceptor is a solid surface. The equation, shown below, results after matching the solution of two problems: a) the flow in the film in which lubrication approximation is assumed, b) the flow in the partially saturated porous material (of thickness, d, saturated up to the pores of radius R_s and with partial saturation permeability k_s), where negligible variation in saturation (ϕ) and Darcyan flow are assumed [1]:

$$\frac{h_\infty}{R_s} = \frac{\chi_{(s)}\cos\theta}{Ca}\left(\sqrt{1+1.34\frac{Ca^{5/3}}{\chi_{(s)}\cos^2\theta}}-1\right) \qquad (1)$$

$$\text{Where } \chi_{(s)} = \left(\frac{L}{d}\right)\frac{k_s}{R_s^{\,2}}$$

Here L is a length scale of the problem, related with the porosities (ϕ), saturation (s) and partially saturated permeability (k_s) of the bulk material ($_1$) and the surface in contact with the glass ($_2$).

$$L = \sqrt{\frac{\phi_1 s_1}{\phi_2 s_2}\frac{k_{s2}\Delta d}{k_{s1}}}$$

EXPERIMENTAL RESULTS AND FITING:

The equation is validated through experiments at different saturations and velocities. Fig 1 show the experimental data on a thick non-woven at two different saturations (the liquid used was a PolyDiMetylSiloxane with 20cp viscosity and 21mN/m surface tension) and a range of velocities covering almost 3 orders of magnitudes (0.1 to 60 cm/s).

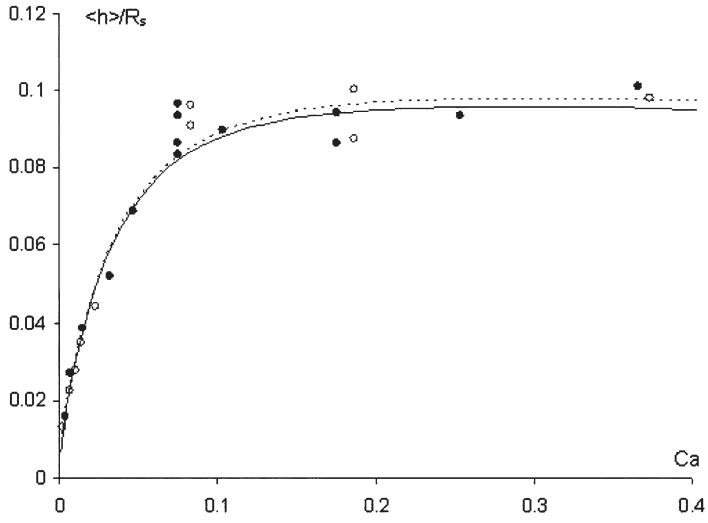

FIG. 1. Best fit curves using (1) and with two free parameters are shown with experimental data. Full symbols represent the higher saturated material (Rs=240μm) and empty symbols the lower (Rs=150μm). The fitting was obtained with : k_{240}=3.9 10^{-6} cm^2 and k_{150}=1.6 10^{-6} cm^2.

The main result indicates that the influence of velocity (indeed the non-dimensionalized velocity, Ca) is important up to a critical value ($Ca_{cr}=\chi^{3/5}$). For higher velocities the thickness of the film decreases so slowly with velocity, that for practical uses, it can be seen as nearly constant (for a certain range of velocities). The "constant" thickness is also characterized by saturation as:

$$h_{\infty_M} = 0.708 \frac{R_s \chi^{2/5}}{Cos^{1/5}\theta}$$

In order to predict the film thickness after wiping, it is necessary to know both the saturation vs pressure and permeability vs saturation curves.

CONCLUSIONS:

We presented here an equation to get the thickness of a film left after wiping. We also showed that the equation fitted very well experimental data ran on a nonwoven for different velocities and two saturations. The equation may be a useful tool to design systems (wipe/lotion) for specific purposes in which wipe's technologies are still not available but desirable (like sun-screen, for example).

REFERENCES:

[1] G. Callegari, A. Baker, K. Zwick, P. Kaplan, A. V. Neimark[4], I. Tyomkin, *PRE,* Wipe Coating, submitted *(2009)*.

BOOSTING OF GLYCERIN HYDRATION IN THE STRATUM CORNEUM

Eric S. Abrutyn*

*Kao Brands, Inc. and *TPC2 Advisors Ltd., Inc.*

As an industry, we strive to develop the best clinically supportive products to help consumers alleviate their skin symptoms. This does not always translate into consumer recognized benefits.

When conducting consumer benchmarking studies with leading moisturizing lotions, the clinically best do not always correlate with higher consumer approval. In fact, sensorial aesthetics play as important a role in consumer judgment of performance as eventual relief of the symptoms. People with very dry skin usually look for a waxy-greasy initial feel that goes on topically heavy and leaves a non-greasy topical feel upon drying. People with normal skin may just want a soft-silky feel with some viscosity/body to the formula when applied, but almost no perceived after-feel when it dries.

Part of the key to balancing skin feel with clinical performance is to manage the way glycerin is delivered to skin during application and shortly after. High glycerin levels translate into better skin hydration but potentially a tack aesthetic, especially in humid environments. Thus, it would be beneficial to understand how to improve on glycerin's clinical performance with less glycerin. From data developed at Kao Brands and published data, we set out to understand if there were better hydrating agents compared to glycerin.

Glycerin has demonstrated its ability as excellent skin hydrating moisturizer ["Ability of Moisturizers to Reduce Dry Skin and Irritation and to Prevent Their Return"; Abrutyn, Simion, Draelos; J.Cosmet. Soc, 56, 427-444 (Nov/Dec 2005)]["Glycerin Moisturizers"; Shaprio, Cosmet. Dermatol., (Suppl Symposium on Cosmetic Efficacy), 26-30 (1996)]. Also, glycerin has been shown to contribute to poor aesthetics because high levels are required for best skin hydration, and thus could lead to low compliance of use.

Data will be presented for various hydrating moisturizers evaluated in different emulsion delivery systems [cationic, gel-emulsion, water-in-silicone, and micro-emulsions] against and in-combination with varying levels of glycerin compared to untreated skin. The tests were run in-vivo, measuring observer dryness, conductance, and tactile sensor at 24 hours, 48 hours and a 7-day regression protocol. Most panel study sizes were between 12-20 people between the ages of 18-65. The specifics on the methodology will not be discussed, but can be reviewed in more detail in the J. Cosmet. Sci., issue 56, pages 427-444 (Nov/Dec 2005) - recipient of Dragoco Award 2002).

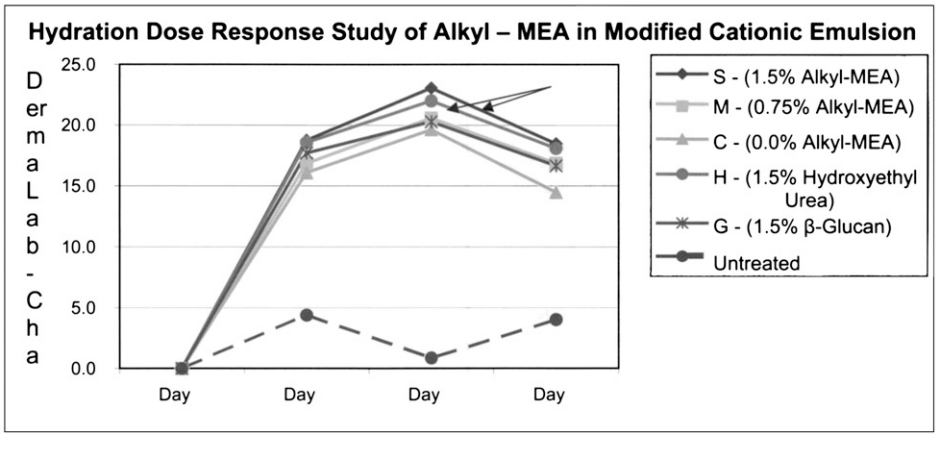

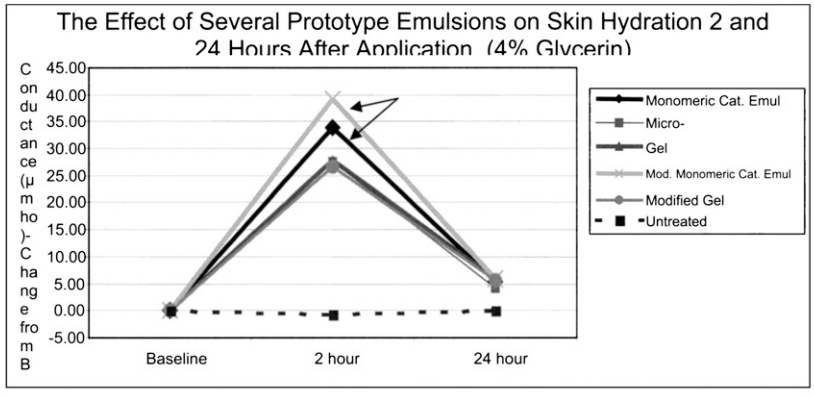

Key observations:

It appears that cationic systems, in particular Behentrimonium Chloride based, produce some of the highest performance hydrating moisturizers when in the presence of glycerin and petrolatum with consumer acceptable soft non-greasy aesthetics.

- Cationic emulsions appear to be a good way to deliver hydrating agents effectively.
- Gel emulsions > Water-in-Silicone >> Micro-Emulsion
- Glycerin = Alklyamide MEA > NaPCA, Hydroxyethyl Urea > all other hydrating agents
- Small amounts of Alkylamide MEA boost performance of Glycerin:
  - ✓ Synergy with Glycerin: Aklylamide MEA's demonstrate superior hydrating efficacy when in the presence of Glycerin
    - lower levels of Glycerin are needed for same hydrating results
  - ✓ Improved reduction in flaking for smoother skin and better aesthetics' of the formula
- More work will be needed to correlate structures of Alkylamide MEA's and skin physiological performance.
  - ✓ Also, there is a need to better understand the skin hydrating mechanics of Alklylamides MEA's

NEW FORMULATION CAPABILITIES USING WATER-IN-SILICONE EMULSIFIERS

Beatrice Durand, Joanna Newton, Cindy Delvalle, Ingrid Vervier and Sylvain Masse

Dow Corning S.A., Europe, Seneffe, Belgium

Introduction

Water-in-silicone emulsions are likely one of the more challenging formulation systems, probably because they are not well known, and studies and literature are limited. This type of emulsion is unique, and specific tools and knowledge are needed for formulation. Factors such as process conditions and addition of an electrolyte to improve stability are familiar. However, some parameters are often overlooked. The first key parameter to consider when formulating a water-in-silicone emulsion is the emulsifier itself. The structure of the emulsifier and its molecular weight are parameters that can influence the characteristics of the emulsion. Organofunctional siloxane polyethers are usually used as emulsifiers, and the examples in this study were polymers with a rake configuration. Other key parameters that impact emulsion stability, and can usually be modified, include the oil phase type, level of emulsifier in the formulation, oil/water phase ratio, and process conditions.

Materials and methods

Silicone-based emulsifiers were compared using a standard evaluation protocol. Oil phase type, emulsifier level, oil/water phase ratio and process conditions were assessed for their influence on emulsion stability and aesthetics.

Three silicone phases were investigated, dimethicone 2 cSt, dimethicone 5 cSt and dimethicone 50 cSt. Two levels of emulsifier, 1 and 2 % actives, were used in the final formulation. The oil/water phase ratios assessed were 40/60, 30/70 and 20/80. Process conditions used in this investigation were based on a regular mixing propeller with or without high shear mixing at the end of the emulsification process.

Several emulsifiers were assessed following this protocol. Among them, some are commercially available, such as *cyclopentasiloxane (and) PEG/PPG-18/18 dimethicone* and *PEG/PPG-19/19 dimethicone (and) C13-16 isoparaffin (and) C10-13 isoparaffin*. Others were experimental systems. The chosen emulsifiers were differentiated by chain length, molecular weight and structure.

Each emulsion was characterized following a unique protocol. Viscosity was recorded after one day and one month with a rheometer (CSL² 500 Carri-Med, TA Instruments, New Castle, DE, USA). Visual stability was recorded at room temperature and 40°C after one day, one week, one month, two months and three months. The emulsions also were observed under a light reflecting microscope at one day and one month.

Results and discussion

The four variable parameters appear to be critical for achieving a successful water-in-silicone emulsion formulation, independent from the emulsifier structure. When the internal phase content of the emulsion is increased, the final viscosity of the emulsion increases. This is also the case if the molecular weight of the silicone phase is increased. To optimize the stability of the emulsion, the level of emulsifier must be increased as the internal phase content decreases. If the level of emulsifier is insufficient, sedimentation eventually occurs. In addition, it is important not to add excessive emulsifier to the formulation. If too much emulsifier is present, the emulsion becomes too viscous for the water phase to be incorporated, or the emulsion can break during or after processing.

The continuous phase also is critical when formulating this type of emulsion. If the molecular weight of the selected silicone phase is too high, the emulsion may break during the emulsification process or shortly afterward. Additionally, if the molecular weight of the continuous phase is too low, sedimentation may be observed after a few days.

If the optimum combination of emulsifier level, type of continuous phase, and oil/water phase ratio is obtained, mixing with a regular propeller should be sufficient to produce a stable emulsion. However, high shear mixing applied at the end of the emulsification process can help improve stability with time. It is important to systematically adjust and observe all these parameters to achieve a stable water-in-silicone emulsion with good aesthetics.

Figure 1 shows a formulating scheme established based on results from this study.

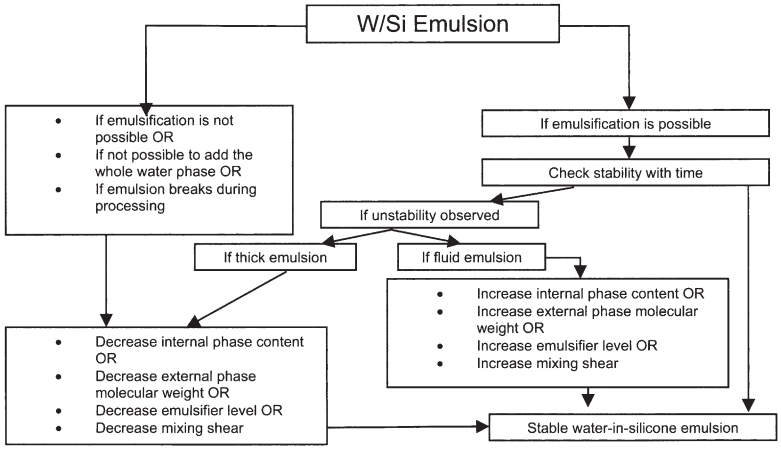

Figure 1. Flowchart for developing water-in-silicone emulsions.

Conclusions

Results of this study provide a tool that can help chemists formulate stable water-in-silicone emulsions. The application of this process helps determine the ideal combination of emulsifier level, type of continuous phase and oil/water phase ratio to achieve good emulsion stability. For example, the combination of 2% active PEG/PPG-19/19 dimethicone (and) C13-16 isoparaffin (and) C10-13 isoparaffin, a 30/70 oil/water phase ratio, and dimethicone 5 cSt produced a pleasant feeling, stable emulsion. This combination was used to formulate a water-in-silicone facial cream called Gleam Dream (Table I).

Table I. Gleam Dream Facial Cream

Ingredients	Wt. %
PEG/PPG-19/19 dimethicone (and) C13-16 isoparaffin (and) C10-13 isoparaffin	4.0
Caprylyl methicone	10.0
Dimethicone, 5 cSt	10.0
C30-45 alkyldimethylsilyl polypropylsilsesquioxane	6.0
Water	61.0
Sodium chloride	1.0
Glycerin	5.0
Actives	1.0
Fragrance	1.0
Preservatives	1.0

SPF RETENTION VIA SILICONE DERIVATIVES

Stacy A. Mundschau, Corey T. Cunningham, Ph.D. and Scott W. Wenzel

Kimberly-Clark Corporation, 2100 Winchester Road, Neenah, WI 54956

OBJECTIVE

Investigate ingredients that may increase the retention of the static sun protection factor (SPF) following water immersion of sunscreen compositions. For alcohol-based sunscreen sprays, the choice of water-resistance ingredients is somewhat limited compared to emulsion systems. To compensate, many products increase the total percentage of active ingredients as they are inherently water resistant. A product that employs a reduced level of actives and an efficient water-resistance system is most desired.

METHODOLOGY

Both in vitro and in vivo SPF measurements were obtained for this research. All in vitro SPF measurements were made using a UV-1000S Ultraviolet Transmittance Analyzer, available from Labsphere (North Sutton, NH) and VITRO-SKIN® synthetic skin substitute, available from IMS, Inc. (Orange, CT). The test protocol used for in-vitro assessments is available from IMS, Inc. In vivo testing was performed by Harrison Laboratories, Inc. of Union New Jersey in accordance with the protocol contained in FDA monograph 21 CFR Parts 310, 352, 700 and 740.

RESULTS

A base set of active ingredients was found to deliver an in vitro SPF value of 50 or greater following immersion. The active ingredient package primarily studied consisted of 7.5% Octinoxate, 5.0% Oxybenzone, 5.0% Octisalate, 4.0% Homosalate, 1.0% Avobenzone and 0.8% Octocrylene. The same active ingredient concentrations were included within the emulsion system with the exception of the Homosalate which was removed. The emulsifying sytem used within this study was a combination of Cetyl Phosphate and Acrylates/C10-30 Alkyl Acrylate Crosspolymer. All alcohol solutions also contained 3.5% Butyloctyl Salicylate. As shown by the graph below, water-resistance efficiencies of greater than 95% were routinely obtained for both systems studied where as a common commercial product containing 29% total active ingredients showed only 63% retention. The addition of 2% of varying silicones including PEG-3 Dimethicone, PEG-12 Dimethicone, PPG-12 Dimethicone, Cyclomethicone and PEG-20/PPG-23 Dimethicone, increased SPF retention of an alcohol solution containing 2% Acrylates/Octylacrylamide Copolymer from 55% to over 80%. Dimethicone derivatives that were both ethoxylated and propxylated were found to be superior to either modification alone.

Specifically, addition of 1% PEG-20/PPG-23 Dimethicone to an alcohol solution containing 2% Acrylates/Octylacrylamide Copolymer was found to retain almost 100% of the original SPF. Solutions containing only 2% or 4% PEG-20/PPG-23 Dimethicone as the water proofing agent were found to retain 83% and 95% of the pre-immersion SPF, respectively.

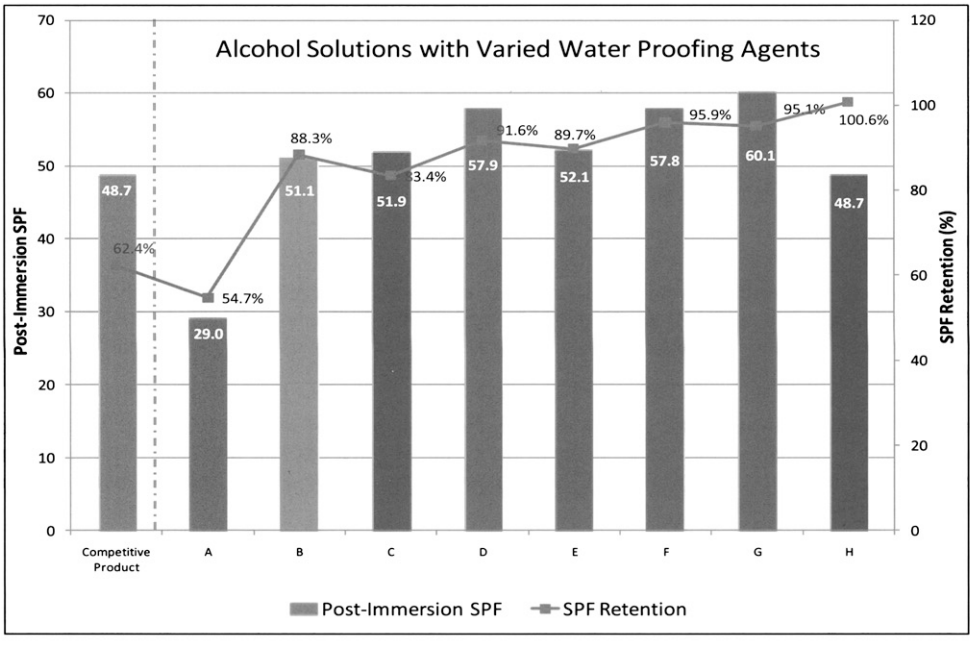

Film formers within the alcohol solutions tested **A.)** 2% Acrylates/Octylacrylamide Copolymer **B.)** 2 % PEG-3 Dimethicone and 2% Acrylates/Octylacrylamide Copolymer **C.)** 2% PEG-12 Dimethicone and 2% Acrylates/Octylacrylamide Copolymer **D.)** 2% PPG-12 Dimethicone and 2% Acrylates/Octylacrylamide Copolymer **E.)** 2% Cyclomethicone and 2% Acrylates/Octylacrylamide Copolymer **F.)** 2 % PPG-23/PEG-20 Dimethicone and 2% Acrylates/Octylacrylamide Copolymer **G.)** 4 % PPG-23/PEG-20 Dimethicone alone and **H.)** 1 % PPG-23/PEG-20 Dimethicone; 2% Acrylates/Octylacrylamide Copolymer

As shown by the Table below, the addition of PEG-20/PPG-23 Dimethicone in a low viscosity (2,500 cP) emulsion improved the in vitro SPF retention compared to Acrylates/C12-22 Alkyl Methacrylate Copolymer.

Total Active Concentration	% PPG23 / PEG-20 Dimethicone	Acrylates/C12-22 Alkyl Methacrylate Copolymer	Static SPF	Post Immersion SPF	SPF Retention
19.3%	0.00	2.00	53.8±2.9	46.5±2.1	86.43
19.3%	2.00	1.00	61.9±3.6	61.2±6.6	98.87
19.3%	2.00	0.00	62.5±3.8	59.2±2.6	94.72

A twenty person clinical conducted on an alcohol formulation containing the combination of PEG-20/PPG-23 Dimethicone and Acrylates/Octylacrylamide Copolymer confirmed in vitro measurements, with the solution achieving an SPF 50 rating under very water resistant conditions.

CONCLUSION

Water soluble and water dispersible silicone polymers can form extremely effective water-resistant films alone or in conjunction with other polymers and has demonstrated efficacy in both alcohol solutions and emulsion systems.

A BETTER UNDERSTANDING OF STRUCTURE-PROPERTIES CONNECTIONS OF THICKENING-STABILIZING POLYMERS

Alicia Roso, Emmanuelle Merat, Olivier Braun and Stephanie Garcel

SEPPIC, 127 Chemin de la Poudrerie, 81100 Castres, France

Keywords : polymer, structure, properties, correlation

(a). **Objective**:

To investigate the correlations between molecular structure of thickening polymers and their final properties in formulations: the thickening effect in challenging pH situations, resistance to UV exposure, and other benefits such as emulsifying-stabilizing capacity of oils without any additional surfactant, texture and sensory profile.

In today's competitive cosmetic market, one of the main challenges is to speed up the product development while maintaining a high quality of work. One way to predict the results and allow a quicker development time is to take advantage of previous experience and develop a better knowledge of the structure-activity connections.

(b). **Methodology**:

The properties of several inverse emulsion polymers (liquid, pre-neutralized, ready-to-use polymers) with various types of monomers, oils and surfactants were analyzed comparatively to a reference polymer in powder form with the same polymer structure.

Tested monomers: Acrylamide, Acryloyldimethyltaurate, Acrylic acid, Hydroxyethylac*rylate*
Tested oils: Dicaprylyl Ether, Hydrogenated polyisobutene, Isohexadecane, Polyisobutene, Squalane
Tested surfactants: PEG-40 Castor oil, Polysorbate 20, Polysorbate 60

Performances of these polymers were then compared in equivalent formulation situations (identical level of active substance or same viscosity):

- Thickening performance was measured as a function of pH in water

- Compared viscosity drop (in %) of the aqueous gels was calculated after UVA and UVB irradiation (20 mJ/cm^2 for each with a sun simulator (Bio-Sun from Vilbert Lourmat Company).

- Maximum % of oil that can be stabilized in a simple cream gel without addition of extra-surfactant (stability after 3 months at R.T. & 1 month at 45°C)

- Gel texture profiles (consistency, pick-up ability) were determined by texturometry analysis using a TEC texture analyzer (from Lamy) following the energy during a compression/traction cycles protocol modeling the action of pick up the product in a standardized packaging).

- Appearance of the gels, ease of picking up, ease of spreading, quick break effect, softness, fresh to rich skin feel & sticky effect were evaluated by sensorial analysis methodology.

(c). **Results**:

Studied properties were influenced by the polymer structure: the monomers, the oil, and the polymer type (inverse emulsion polymer or powder). The surfactant chemistry did not appear as a significant parameter in this study.

The monomer choice was found as the key parameter to get a constant thickening effect in a wide pH range and an improved resistance of the gel to UV exposure: using Acrylamide and Acryloyldimethyltaurate as major monomers allowed to formulate from pH 3 to 10 and the gels keep stable after UV exposure while formulation below pH 5.5 was not permitted with acrylic acid and the gels were destabilized by UV irradiation.

Conversely, the ability to stabilize high levels of oils without addition of extra-surfactant mostly depends on the polymer type (liquid or powder): polymers in inverse emulsion stabilize high quantity of oils: 40 to 45% of C8/C10 triglyceride and more than 15% of mineral oil whereas the reference powder polymer only allowed to stabilize respectively 10% and less than 5%. The nature of the oil present in the inverse emulsion polymer had also a high impact with respect to paraffin oil stabilization: Isohexadecane gave the best result.

For some other properties, such as texture and sensorial profile, the connections were found to be more complex and would require further investigations. For instance, polymers in inverse emulsion provided globally supple and easy to pick up gels as the reference powder polymer gave stiffer and less easy to pick up gel. Once again, a better pick up ability was achieved when using Acrylamide or Acryloyldimethyltaurate as major monomers compared to Acrylic acid.

(d). **Conclusion**:

The study of the structure-properties connections gave very interesting tools for the development of new thickening polymers with improved technical performances and tailored sensory profiles.

CHARACTERIZATION OF HAIR DAMAGE AND ITS EFFECT ON HAIR COLOR FADING AND THE ROUTES FOR COLOR PROTECTION FROM SHAMPOO STRIPPING

Yan Zhou, Linda Foltis, David J. Moore, Ph.D., Ray Rigoletto, Wosson Solomon, Grisel Tumalle and Xin Qu

International Specialty Products, 1361 Alps Road, Wayne, NJ 07470

INTRODUCTION

Hair damage through chemical, thermal-mechanical treatments is a significant factor contributing to hair color fading of dyed hair. Faster color fading of damaged hair leads to more frequent re-coloring hair therefore to further damage and accelerated fading. Consumers want to maintain the vibrancy of the color until the next oxidative process. This translates to protecting hair color from fading for up to six weeks when color will need to be refreshed as noticeable re-growth will need to be colored. Therefore, there is a market need for treatment solution that is effective for preventing fading or increasing color longevity of damaged hair which the consumers often have when they use chemical treatment frequently such as coloring or bleaching. Color protection is now considered to be an important area in hair care market (1, 2, 3). To meet this market need, knowledge on understanding of the chemical and physical changes of damaged hair is needed. Therefore, the objectives of this work are to understand the damaged hair substrate and the effect of hair damage on color fading, and to develop routes for color protection for damaged hair.

METHODOLOGY

A novel technique, FTIR spectroscopic image analysis (4), was used to characterize compositional changes of chemically damaged hair fibers. Water contact angle measurement, AFM, DSC and water sorption measurement were used to measure other property changes of damaged hair and treated hair. Measurement techniques for evaluating color change of dyed hair samples from color fading tests include colorimetric measurement; quantitative digital image analysis on color darkness, correlating with Salon tests with mannequins of human hair and subjective panel studies to link to the consumer perceivable changes.

RESULTS AND DISCUSSION

FTIR Image analysis of hair fiber cross sections indicates that there are significant reduction of protein and lipid contents in triple bleached hair and alkaline treated hair, by 26% and 29%, respectively, compared with virgin hair, as shown in Fig.1. FTIR image analysis also indicates that there are 59% and 33% increases of cysteic acid for bleached hair and alkaline treated hair, respectively, compared with virgin hair. AFM analysis shows that the damaged hair (triple bleached) surface contains micropores. The measured contact angle of the triple bleached hair is 41°, compared with 81° for the unbleached hair, indicating that the surface of damaged hair is more hydrophilic. These structural degradations in chemically treated hair fibers promote color fading. In addition, disulfide bond cleavage by reducing agents significantly increases color fading. Fig.2 shows color fading test results of dyed bleached hair from 10 time shampoo washing, indicating that hair color loss increased by one fold from one hour bleaching to two hour bleaching and by an additional 25% increase with 3 hour bleaching. In addition, dyed bleached European hair fades much more than dyed bleached Asian hair, especially with deeply bleached hair. One of the anti-fading approaches developed for damaged hair is to seal or reduce the micropore openings on cuticle surface and in the meanwhile provide a substantive hydrophobic barrier on hair surface, therefore, prevent the dye from washing out. Towards this approach, the copolymer of vinylpyrrolidone, dimethylaminopropyl methacrylamide, and methacryloylaminopropyl lauryldimonium (INCI- Polyquaternium-55) is found to be very effective. Fig.3 shows that the Polyquaternium-55 (PQ-55) anti-fading treatment system provides as high as 48% protection over the untreated control for dyed, triple bleached hair. The anti-fading efficacy seems to increase with the degree of hair damages. The anti-fading system was proved to be effective for both dyed bleached Asian and European hair. The bleached hair fibers after multiple treatments with PQ-55 and multiple washes with SLES have the water contact angle increased from 41° to 64°. Fig.4 shows the hair image analysis results and pictures of dyed bleached Asian hair after 10x washes and treatment from different treatment regimens containing PQ-55, proving that the combined treatment of leave in gel and rinse off shampoo formula is the most effective treatment.

CONCLUSION

Both chemical and physical changes of damaged hair were determined and the effect of hair damage from chemical treatment on color fading was measured quantitatively. Approaches for color protection of damaged hair are developed. The anti-fading system containing Polyquaternium-55 is proven to be effective in preventing color fading of damaged hair in both leave in and rinse off treatment systems and provides significant less "off shade" fading than a number of existing commercial benchmarks tested.

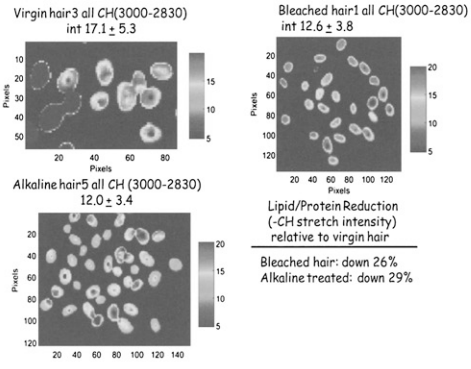

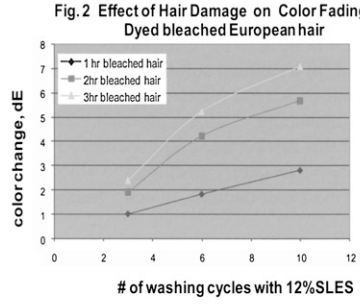

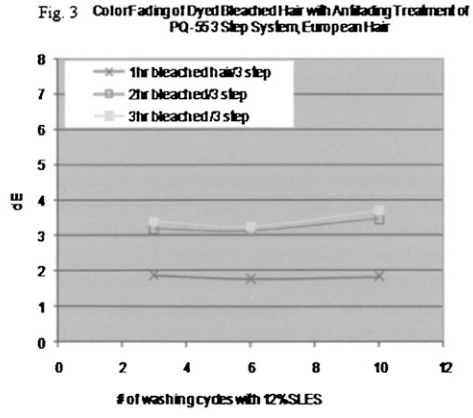

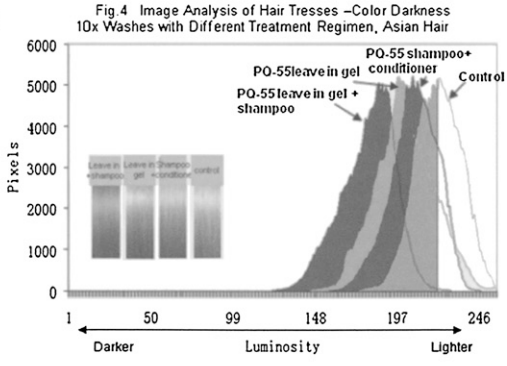

REFERENCE

1) B. Brewster, Color lock in hair care, *Cosmet. Toilet.,* **121** (3), 28-36 (2006)
2) Ch. Fox, Careing for color-treated hair, *Cosmet. Toilet.,* **120** (11), 36-43 (2005)
3) G. Wis-Surel, Some challenges in modern hair color formulations, *Int. J. Cosmet. Sci.*, **21**, 37-340 (1999)
4) R. Mendelsohn, H.-C. Chen, M.E. Rerek, D.J. Moore, Infrared microscopic imaging maps the spatial distribution of exogenous molecules in skin, J. Biomed. Opt. 8 (2003) 185–190.

FLOW CELL MICROSCOPY: A NOVEL METHOD TO VISUALIZE PRODUCT DEPOSITION ON HAIR

Renee Bolden[1], Ph.D., Dirk Domaschko[1], Julie Lubbers[1], Jeni Thomas[1], Ph.D., Mark Brown[1], Marge Peffly[1], Ph.D. and Yujun Li[2], Ph.D.

[1] *The Procter & Gamble Company, Sharon Woods Innovation Center, Cincinnati, OH*
[2] *The Procter & Gamble Company, Beijing Technical Center, China*

Background

Understanding the mechanism of action for the deposition of hair care ingredients is important for developing effective formulations. Common deposition mechanisms of action include 1) deposition via adhesion to the hair surface, 2) deposition via filtration due to fiber interaction/tangling and 3) deposition via surface modification. Historically, ingredient deposition has been investigated using bulk extraction methods. The total amount deposited on the hair is then correlated to scanning electron microscopy images to develop an understanding on how new formulations provide conditioning benefits. In order to better understand product performance, we have developed the Flow Cell Microscopy method to visualize deposition in real-time.

Flow Cell Microcopy is a novel method, utilizing a commercially available Focht Flow Cell to visualize deposition of shampoo and conditioner ingredients onto a hair fiber. Product usage is simulated by passing a solution of diluted formula through the flow cell (shampoo or conditioner usage phase) followed by distilled water (rinse phase). Single or multiple hair fibers are trapped within two gaskets located in the flow cell. The deposition mechanism of action, whether via filtration or via adhesion, can be better understood through the use of the modified flow cell. It was found that separating the hair fibers from the cover slip is important to enable laminar flow across the hair fiber and to avoid deposition via entrapment between the coverslip and hair. The interaction of ingredients with hair is captured via a Zeiss compound microscope used in bright field mode at a magnification between 50-200x. Dynamic videos showing real-time deposition on hair are created using a digital camera with streaming capture capability. For complimentary information, the hair that was "washed" within the flow cell can be examined using scanning electron microscopy for correlation back to historical bulk measurements.

Figure 1

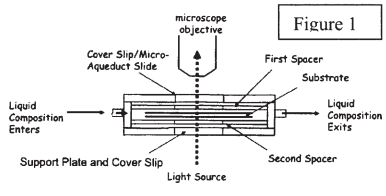

Results

In our research we used flow cell microscopy to evaluate the deposition of shampoo polymers (guar hydroxypropyltrimonium chloride, poly-diallyldimethyl ammonium chloride (poly-DADMAC) and polyquaternium-76/Triquat-76) and conditioner ingredients (behetrimmonium chloride, stearyl ethylhexl dimonium methosulfate, behetrimonium methosulfate, PDMS and bisaminopropyl dimethicone) on hair in order to better understand the deposition mechanism.

Three results were observed for shampoos: 1) ingredients adhere to the hair during the treatment phase and remain adhered during the rinse phase (deposition via adhesion), 2) ingredients adhere to the hair during the treatment phase and are released during the rinse phase (deposition via filtration) and 3) no ingredient interaction with the hair during treatment or rinsing phase (deposition via filtration).

Interactions between a Triquat-76-containing coacervate and PDMS illustrate the ability of flow-cell microscopy to visually elucidate deposition mechanisms. Figure 2 shows still images obtained for the shampoo and rinse phases for the Triquat-76 containing shampoo. Bulk silicone measurements show that silicone deposition was 576µg/g on virgin hair. However, when bleached hair was treated with the same Triquat-76-containing shampoo, the bulk deposition value for silicone was reduced to 31µg/g on hair. This change in deposition can be seen in Figure 3 where silicone is no longer observed adhered to the hair shaft. Therefore it was concluded that Triquat-76 is a possible technology for hair that responds well to deposition via adhesion and not suitable as a technology capable of surface modification for color-treated hair.

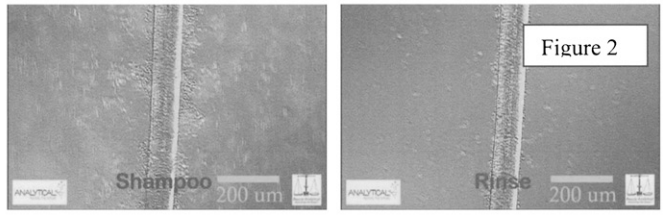

Figure 2

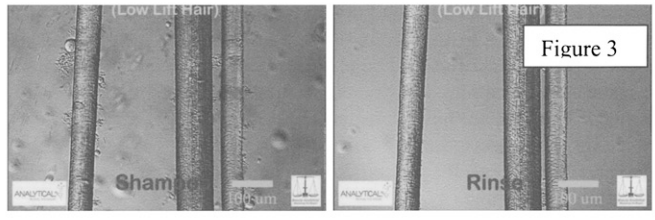

Figure 3

Deposition via filtration was also observed with flow cell microscopy using guar hydroxypropyltrimonium chloride, as shown in Figure 4. Within the flow cell, two fibers were positioned close to each other, and deposition was observed between the hair fibers during the shampoo and rinse phases with little to no deposition observed on the outer edges of the hair fibers. This occurrence was an indication of deposition via filtration rather than the adhesion mechanism. Therefore, hydrolyzed guar was determined to be a hair care technology suitable for hair types that could filter conditioning ingredients.

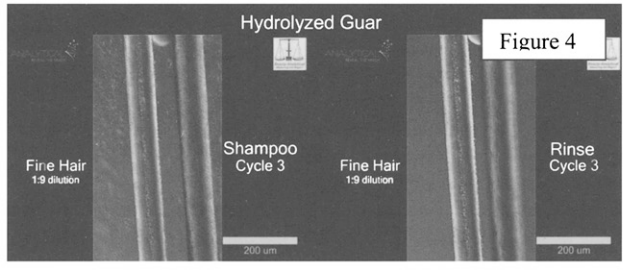

Figure 4

Two results were observed for conditioner formulations: 1) ingredients adhere to the hair during the treatment phase and increase during rinsing (heavy deposition via adhesion) and 2) ingredients adhere to the hair during the treatment phase and mostly rinse away during rinse phase leaving a thin layer on the hair (light deposition via adhesion). Mechanistic understanding of light and heavy depositing conditioner formulas can help design formulas suited to fine hair consumers needing light conditioning versus thick and curly hair consumers, which often needs heavier conditioning.

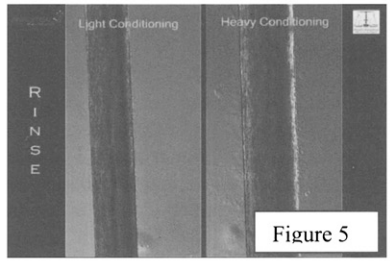

Figure 5

Flow cell microscopy has proven to be an invaluable tool to understand how different hair care formulations deposit and relate the results to specific consumer needs. It is envisioned that this method can be applied in other areas such as personal cleansing moisturization deposition and laundry detergent deposition.

EFFECT OF NATURAL PROTEINS AND PROTEIN HYDROLYZATES ON HAIR ELECTROKINETICS AND WETTABILITY

Janusz Jachowicz[2], Ph.D., Susan Daly[1], Ph.D., Robert Bianchini[1], Ph.D., and Thomas Polefka[1]

[1]*Johnson & Johnson*
[2]*Better Cosmetics, LLC*

Peptides, proteins and their hydrolyzates are widely used in hair and skin care formulations [1,2]. The most commonly used materials are hydrolyzates derived from animal and vegetable sources such as keratin, collagen, elastin, silk, soy, corn, wheat, etc. Natural, unadulterated proteins are used less frequently. The affinity of proteins or protein hydrolyzates to hair and their ability to modify the fibers is related to their native chemical composition, molecular weight and any additional chemical modifications. Others have performed quantitative analysis of sorption on hair [3-9].

The present work concentrates on the analysis of protein-hair interactions by using surface techniques such as streaming potentials and contact angles. Streaming potential analysis was carried out in an instrument that can simultaneously measure electrokinetic and permeability parameters of hair plugs during real-time treatment with cosmetic raw materials [10]. Electrokinetic data can reveal protein adsorption/desorption kinetics on hair and can be used to estimate protein affinity to hair based on the change in the zeta potential value of hair before after treatment. Permeability data can indicate the thickness of the layer deposited onto hair. For deposition systems that do not affect the surface charge properties, contact angle analysis provides an alternate means to evaluate deposition based on surface wettability changes.

Streaming potential and/or contact angle measurements reveal that the adsorption and desorption behavior of a variety of materials, including wheat and soy hydrolyzates, lysozyme, avidin, and albumin, were found to vary significantly on the hair surface.

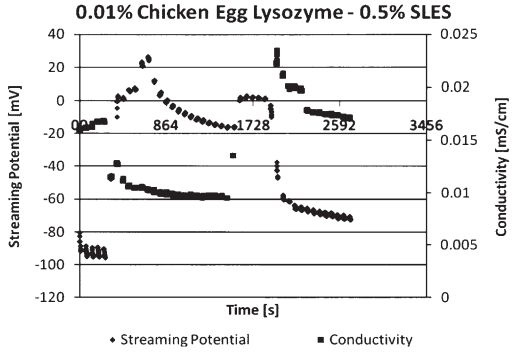

Figure 1 Streaming potential and conductivity as a function of time for the following sequence of treatments: (1) 5 measurements of untreated hair, (2) 5 cycles of treatment with 0.01% Lysozyme, (3) 15 measurements with $5 \cdot 10^{-5}$M KCl, (4) 5 cycles of treatment with SLES, and (5) 15 measurements with $5 \cdot 10^{-5}$M KCl.

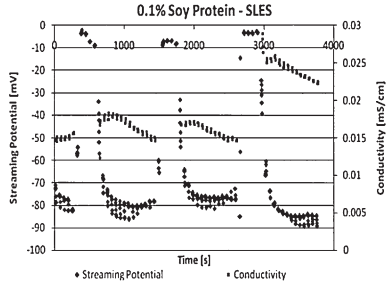

Figure 2 Streaming potential and conductivity as a function of time for the following sequence of treatments: (1) 5 measurements of untreated hair, (2) 5 cycles of treatment with 0.1% Soy protein hydrolizate, (3) 15 measurements with $5 \cdot 10^{-5}$M KCl, (4) 5 cycles of treatment with 0.1% Soy protein hydrolizate, (5) 15 measurements with $5 \cdot 10^{-5}$M KCl, (6) 5 cycles of treatment with SLES, and (7) 15 measurements with $5 \cdot 10^{-5}$M KCl.

Figure 1 presents the streaming potential and conductivity data obtained for virgin hair treated with lysozyme and subsequently with sodium lauryl ether sulfate (SLES). The results show the binding of the protein to hair, accompanied by an increase in streaming potential (as compared to untreated hair) and a decrease in conductivity, probably due to neutralization of charge on the surface of hair. Subsequent treatment with SLES removes most of the adsorbed lysozyme and increases the conductivity, probably because of adsorption and slow desorption of the anionic surfactant. In contrast to this, the streaming potential change of hair upon treatment with soy hydrolyzate is negligible and this protein does not show reduce the hair's conductivity (Figure 2). The application of SLES significantly increases the plug conductivity.

The results of electrokinetic analysis of hair are complemented by the measurements of contact angles, which can detect variations in hydrophilicity/hydrophobicity of various types of hair as a result of adsorption of proteins. For example, it was observed that hydrolyzed wheat and soy proteins increase the advancing contact angle of bleached hair (making it more hydrophobic) and decrease the advancing contact angle of intact hair (thus, making it more hydrophilic).

The paper will also discuss the use of wettability and streaming potential methods to follow the changes on the surface of hair as a result of multiple treatments involving proteins, polymers, and surfactants.

References

1] - V.L.Johnson, Proteins in cosmetics and toiletries, Drug Cosmet. Ind., 126(6), 36-39, 136-137 (1980).
[2] - M.Chvapil and Z.Eckmayer, Role of protein in cosmetics,Int.J.Soc.Cosmet.Sci.,7,41 (1985).
[3] - S.A.Karjala, J.E.Williamson and A.Karler, Studies on the substantivity of collagen derived polypeptides to human hair, J.Soc.Cosmet.Chem.,17, 513 (1966).
[4] - S.A.Karjala, A.Karler and J.E.Williamson, The effect of pH on the sorption of collagen-derived peptides by hair, J.Soc.Cosmet.Chem.,18, 599 (1967).
[5] - E.S.Stern and V.L.Johnsen, Studies on the molecular weight distribution of cosmetic protein hydrolisates, J.Soc.Cosmet. Chem., 28, 447 (1977).
[6] - A.Turowski and B.C.Adelmann-Grill, Substantivity to hair and skin of 125-I-labelled collagen hydrolisates under application simulating conditions, Int.J.Soc.Cosmet. Sci., 7,71 (1985).
[7] - G.R.Mintz, G.M.Reinhart and B.Lent, Relationship between collagen hydrolisate molecular weight and peptide substantivity to hair, J.Soc.Cosmet.Chem.,42,35 (1991).
[8] - Y.Peng, V.Glattauer, J.A.Werkmeister, J.A.M.Ramshaw, Evaluation of collagen products for cosmetic application, J.Cosmet.Sci.,55, 327 (2004).
[9] - S.D.Coapman, J.L.Lichtin, A.Sakr, and J.R.Schiltz, Studies of the penetration of native collagen, collagen alpha chains, and collagen cyanogens bromide peptides through hairless mouse skin in vitro, J.Soc. Cosmet. Chem., 39, 275 (1988).
[10] – J.Jachowicz, C.Williams, and S.Maxey, Sorption/desorption of ions by dynamic electrokinetic and permeability analysis of fiber plugs, Langmuir 9 (11), 3085 (1993).

QUANTIFICATION OF FIBER FRAGMENTATION OF HAIR THROUGH COMBING AS A MEASURE OF THERMAL PROTECTION

Ray Rigoletto, Jadwiga Karolak and Don Koelmel

International Specialty Products, 1361 Alps Road, Wayne, NJ 07470

Introduction

Styling appliances such as curling and hot flat irons have grown in popularity in recent years. An increased use of hot flat irons, which can typically exceed 200 °C, have followed consumer trends for straight hair styles. With continued use at this extreme heat, the consumer quickly realizes the damaging effects to their hair. As a result, an increased number of styling products claiming thermal protection are continually being launched to the market. In response, a need has developed in our industry for new compositions with improved thermal protective features as well as viable methods that substantiate their efficacy.

Objectives

This study presents a method that can be used to test the ability of a composition to provide thermal protective effects against the excessive heat applied to hair from hot flat irons by measuring the reduction in fiber fragmentation after a controlled combing process. The validity of the method is shown by highlighting the importance of the combing process in the test method which imparts realistic stresses on the hair, generating thermal protective data on two polymers that have historically been shown to provide thermal protection from curling irons [1], and utilizing analytical techniques to back up the reduction in fiber fragmentation data. Mechanisms of action of the thermal protective effects are proposed.

Methods

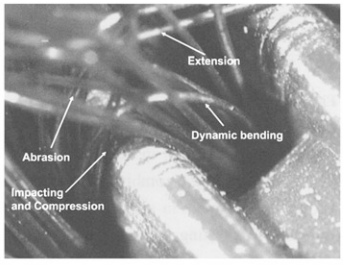

Figure 1-Various stresses during combing

The advantage of the fiber fragmentation method is based on the fact that combing provides realistic stresses on the hair that are evident in hair styling. It has been proposed by Swift [2] and later by Robbins [3] that hair does not fracture solely by tensile stresses. Besides extension, there are various types of strain that are responsible for the fracture and ultimately the breakage of hair. As seen in Figure 1, these include shear forces within the cortex, the impacting of one hair fiber over another, compression, extension of the fiber, rate of extension and abrasion. The quantification of fiber fragmentation can then be used as a measure of the alleviation of weakening of the hair by the thermal protective composition.

The treatment schedule is depicted in Figure 2 which shows in schematic form the steps involved in treating the hair both with the protective composition as well as exposure with the thermal appliance. The hot flat ironing process consists of slowly pulling the appliance down the tress in the course of 12 seconds. This procedure is repeated five times for a total exposure time of one minute and then the tress is allowed to cool. This one minute heat treatment is repeated throughout the course of the treatment schedule. At the end the hair is washed with 12% Sodium Laureth Sulfate to remove any protective composition remaining on the hair so that the reduction of fiber fragments after combing is attributed to the protection afforded to the hair and not to the direct conditioning properties of the composition.

After combing, fiber fragments collected underneath the tress are fixed to a plastic sheet so that the broken fibers can be easily numbered. Percent reduction in hair breakage is calculated based on appropriate controls. Prior to the first shampoo and after the final shampoo before combing, hair is analyzed using scanning electron microscopy, emission due to tryptophan with a spectrofluorometer [4] and heat absorption with a differential scanning calorimeter (DSC) [5].

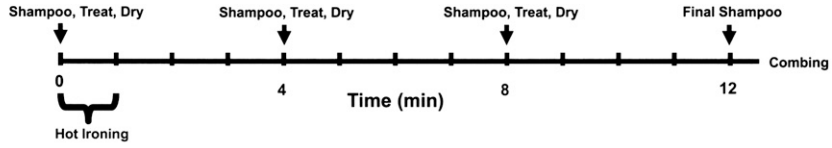

Figure 2-Treatment schedule

Results

Reduction in hair breakage during combing was achieved by polymer pretreatments to hot flat ironing set at a temperature of 205 °C; Figure 3. Results from instrumental techniques also show positive protection afforded by the pretreatments. These include a reduction in tryptophan degradation and noting the reduction of severe morphological changes of the fiber surface using SEM. DSC shows that protection is not just localized at the surface but also includes the cortex; results in Figure 4. Protection to thermal insult is also evident at a hot iron setting of 232 °C.

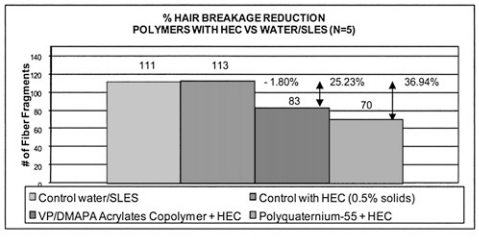

Figure 3- Percent thermal protection from polymers incorporated into a solution of hydroxyethylcellulose

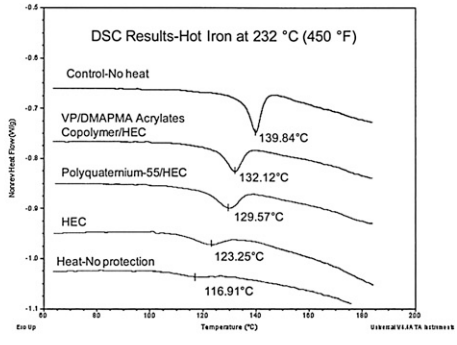

Figure 4-DSC Results

Conclusions

Quantification of fiber fragments after a controlled combing process can be used to measure the alleviation of weakening to hair from hot flat ironing by a protective composition. An important factor in this method is the mechanism of breakage and the type of stresses that are imparted to the hair during the combing process. The method is confirmed by showing positive results on two thermal protective polymers in simple as well as in formulated systems and confirmatory results from instrumental techniques. This testing strategy can be utilized for future research for exploring the mechanism of thermal protection of hair and an understanding of the necessary components in the design of new protective compositions.

References

1. McMullen, R., Jachowicz, J., Thermal degradation of hair. II. Effect of selected polymers and surfactants, J. Cosmet. Sci., 49, 245-256, (July/August 1998).
2. Swift, J.A., The mechanics of fracture of human hair, International Journal of Cosmetic Science, 21, 2227-2239, 1999.
3. Robbins, C., Hair breakage during combing. I. Pathways of breakage, J. Cosmet. Sci., 57, 233-243, (May/June 2006).
4. Jachowicz, J., et al., Photodegradation of Hair and its Photoprotection by a Substantive Photofilter, DCI Magazine, December 1999.
5. Wortmann, F.J., et al., Investigations of cosmetically treated human hair by differential scanning calorimetry in water, J. Cosmet. Sci., 53, 219-228, (July/August 2002).

SYNCHROTRON X-RAY TOMOGRAPHY OF AFRICAN-AMERICAN HAIR REVEALS A REDUCTION IN FIBER ENERGY ABSORPTION AS A RESULT OF 2.5% NaOH RELAXER TREATMENT

Guive Balooch, Ph.D., Crystal Porter, Ph.D. and Harold Bryant, Ph.D.

L'Oreal Institute for Ethnic Hair and Skin Research, Chicago, IL

Introduction

Approximately 70% of African-American women straighten their hair using relaxers since the inherent state of the hair can have a high degree of curl that is often difficult to manage [1, 2]. While it has been shown that this treatment can compromise the overall strength of African-American hair [3], the nature of the modification of protein in hair with relaxer treatment has not been studied extensively due to lack of high-resolution techniques. Furthermore, along the same line of reasoning, little is known about the effect of relaxer treatment in influencing the three-dimensional localized fractography of hair.

In this study, a non-destructive and high spatial resolution (750 nm) approach of synchrotron x-ray tomography was utilized to assess the 3-dimensional fractography and energy absorbance of hair fibers. The exploration of this novel technique to understand the effect of relaxer treatment on African-American hair fibers has shown, for the first time, the differences in the 3-dimensional fractography and energy absorption of hair fibers as a result of treatment with nanometer spatial resolution. These results have revealed a new insight into how African-American hair treatments influence energy absorption and structural properties, which may ultimately, influence hair breakage.

Methods

X-ray tomography imaging was performed at the Advanced Light Source on Beamline 8-3-2 at the Lawrence Berkeley National Laboratory by obtaining two-dimensional radiographs as the hair fibers were rotated through 180˚ in 0.5˚ increments (Fig. 1). The radiographs were reconstructed into 2,500 to 5,000 slices by Fourier-filtered back projection with a 1 um resolution. The attenuation coefficient (mm^{-1}) of each pixel is represented by the false colors and relates to the protein concentration. A detailed description of synchrotron x-ray tomography and data analysis can be found in previous publications [4]. Five hair fibers were imaged per sample where virgin hair fibers were imaged first, then subsequently relaxed with a 2.5% NaOH simplex solution for 15 minutes (20^0C), and imaged again to investigate differences.

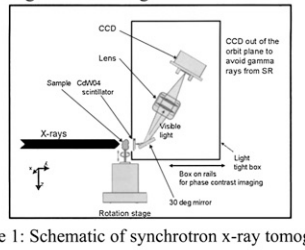

Figure 1: Schematic of synchrotron x-ray tomography

Results

Synchrotron x-ray tomography revealed a significant reduction (45%, $p<0.01$) in fiber energy absorption of the entire fiber (cuticle and cortex) as a result of NaOH treatment [Figure 2a]. This decrease in energy absorption as a result of relaxer treatment is consistent with changes in other physical property measurements observed in the literature, such as a decrease in tensile properties as well as a decrease in thermal properties [3]. Three-dimensional tomographic reconstructions demonstrated cross-sectional [Figure 2b] and longitudinal crack formation [Figure 2c] in the

treated fibers. To investigate the surface deformations, the cortex region was subtracted using the reconstructed software, leaving only the cuticle region [Figure 2c]. Significant geometric difference were observed, where the NaOH treatment induced morphological surface deformations to the hair fiber compared to virgin [Figure 2c].

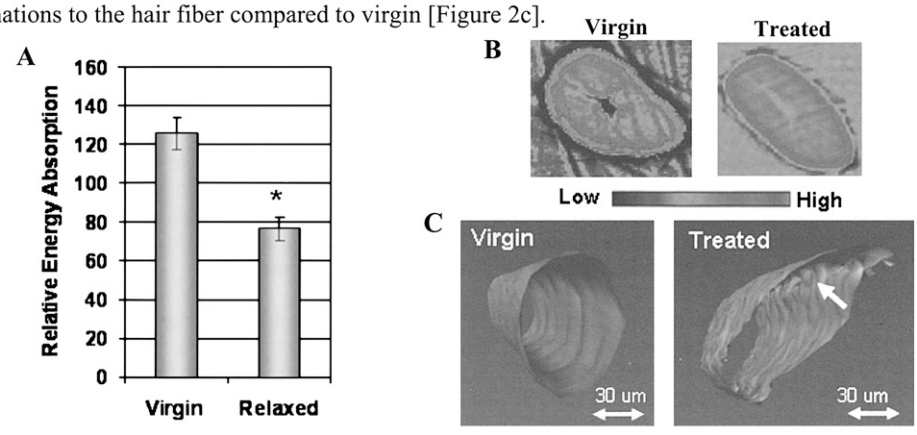

Figure 2: (a) Quantitative 3-D data (mean +/- standard deviation) extraction of over 5,000 slices revealed a significant reduction in energy absorption of the entire fiber (cuticle and cortex) with relaxer treatment compared to virgin. * represents $p<0.01$ using a student t-test. (b) Sample cross section slices chosen from over 5,000 generated slices revealed a reduction in energy absorption with relaxer treatment. (c) Three dimensional XTM reconstructions of the cuticle of a virgin hair fiber and the same fiber treated with 2.5% NaOH. Significant macro and micro-structural differences were seen with treatment, including micro-cracks along the fiber as indicated with the white arrow.

Conclusion

Here the influence of relaxer treatment on the structural properties of African-American hair was explored. While specific proteins have not been identified in hair by synchrotron tomography; they have been identified in other tissues such as bone [4]; and therefore, the local energy absorption values can eventually be correlated to the presence of protein. By using synchrotron x-ray tomography, we were able to show that relaxer treatments reduce the local energy absorption and increase micro-fractures and deformations; which can ultimately; compromise the macroscopic properties of African-American hair. These results have revealed, for the first time, a unique way to study 3-dimensional fractography at a local scale and how relaxer treatments modify hair. Therefore, this may lead to a better understanding of how current and new treatments can be improved by modifying the surface and internal properties of hair during and after treatment to reduce hair breakage. This technique also has the potential to assist in understanding the influence of relaxers on specific areas along the length of the fiber such as kinks and twists, which may impact mechanical integrity.

References

1. Robbins, CR. *Physical Properties and Cosmetic Behavior of Hair, Chemical and Physical Behavior of Human Hair*, New York, Spring-Verlag, 1988.
2. Syed, A. et al. *Cosmetic & Toiletries* 1995; **110**: 39
3. Franbourg, A. et al. Current Research on ethnic hair. *J. Am. Acad. Dermatol.* 2003; **48**: 115
4. Balooch, G. et al. TGF-beta regulates the mechanical properties and composition of bone matrix. *Proc Natl Acad Sci* U S A. 2005 Dec 27;102(52):18813-8. Epub 2005 Dec 14

HAIR BREAKAGE FOR THE AFRICAN-AMERICAN CONSUMER: CAUSES AND CONSUMER PERCEPTION

Bradford Pistorio[1], Ph.D., Grace Yang[1], Stephane Diridollou[1], Ph.D., Philippe Hallegot[2], Ph.D., Alejandra Camacho[1], Ph.D., Nestor J. Zaluzec[3], Ph.D., Felicia Dixon[1], Ph.D., Crystal Porter[1], Ph.D. and Harold Bryant[1], Ph.D.

[1]L'Oreal Institute for Ethnic Hair and Skin Research, Chicago, IL
[2]L'Oreal Research Department of Physics, Aulnay, France
[3]Electron microscopy Center, Materials Science, Div. Argonne National Lab, Argonne, IL

Introduction

A consumer study was performed at the L'Oréal Institute for Ethnic Hair and Skin Research in Chicago to gain perspective of what hair breakage means to the consumer. From this study, we have confirmed that the most prevalent hair concern for the African-American female is hair breakage for either natural or chemically treated hair. Grooming habits as well as chemical treatments, heat application, or other styling products that could contribute to breakage were also addressed during the survey. Overall, this study has allowed us to develop laboratory experiments to begin to understand hair breakage and to address these consumer concerns.

The purpose of our work is to understand the hair breakage process and the influence of chemical treatments on hair breakage. Toward this end, we have implemented a combination of techniques to characterize the mechanical properties of hair and to understand the morphological features that may contribute to breakage. Hair was collected from individuals who perceived that their hair was prone to breakage and was analyzed using miniature tensile testing (MTT). Additionally, an environmental scanning electron microscope (ESEM) was used to identify when and how hair breakage occurs with curly virgin hair fiber. An advantage of the ESEM is that hair can be imaged at high magnification in real time with variations in heat, humidity, and chemical treatments under mechanical stress to emulate ambient conditions.

Methods

A consumer survey was conducted on 715 African-American panelists in Chicago. In a separate study, hair samples were collected from twenty-six individuals who perceived their hair as having high breakage. Virgin hair was also used in this study as a basis for comparison. Experiments were carried out in a FEI Quanta 400 FEG-ESEM operating both at the Institute and in the Electron Microscopy Center at Argonne National Laboratory.[1] Secondary electron images were taken at 15 to 25 kV with temperature variations from 1 to 200 °C and relative humidity (RH) variations from 1% to 100%. Specimens were carefully attached to specific ferrules and affixed to a custom built tensile testing stage by Gatan, Inc. for the dynamic investigation of single hair fibers, utilizing 2 and 5 N full scale load cells. Contrast enhancement and measurements were performed using Image J. The tensile properties of dry hair from subjects were determined using a Dia-Stron Ltd. Miniature Tensile Tester 675. The environmental temperature and humidity were 22 ± 2 °C and 45 ± 5% RH, respectively. All tensile properties were measured on the first 50 hair fibers that exhibited normal failure profiles. Young's modulus and break stress were normalized using the cross-sectional area of each fiber measured with a laser micrometer.

Results and Discussion

The Institute in Chicago has established an ethnically diverse consumer database that has allowed us to gain insight into the African-American consumer. Particular to our research goals, we conducted a survey focused on hair breakage. Within this study, 95% experienced hair breakage, while 64% regarded hair breakage as a problem. Hair breakage was highly related to "split ends" and "hair shedding," in which most of the respondents noticed breakage during combing and brushing. Among those surveyed, 90% had some chemical treatments on their hair with 79% being relaxer. Breakage was also noted upon usage of heat appliances, such as blow-dryers and curling irons. Of those surveyed, 87% attempted to alleviate their concerns with 71% claiming the actions they took remedied the problem. Some of the most commonly used products included oils, conditioners, and moisturizers. Consumers also attempted using less heat, altering products, trying new anti-breakage products or just going natural.

Concurrent to this study, post-mortem hair fibers were collected from twenty-six individuals who experienced hair breakage for mechanical and microscopic analysis. The collected hair ranged from natural to a variety of chemical treatments, including lye, no-lye and color. ESEM images of the hair revealed cracking and wearing patterns associated with breakage. Preliminary results from MTT also demonstrated that these samples had comparable

mechanical properties to laboratory treated hair. The collected fibers that contained chemical treatments had an average break stress (BS) value of 137.9 ± 25.3 MP, which was comparable to laboratory lye-treated hair (BS = 137.01 ± 16.39 MPa) versus no-lye samples (BS = 104.97 ± 20.95 MPa). As a point of reference, virgin hair samples had an averaged BS of 189.93 ± 19.52 MPa.

In order to further understand the causes of breakage due to inherent weak points in hair, we examined single fibers under mechanical stress with high resolution ESEM using a tensile testing stage. Images of an uncoated hair fiber were taken along the axis of the fiber under constant conditions and are shown in Figure 1 a - c. Initially, the appearance of cracks was observed at the hair surface, followed by the extension of the crack perpendicular to the fiber axis. The cracks on the cuticle in both the transverse and longitudinal directions, as well as the distribution of the breakage on the cortex, were observed progressively until the cortex completely fractured (Figure 1d). During this experiment the separation of the cuticle from the cortex occurred upon a mechanical stress, suggesting a weakness between these two structures that may be related to the mechanical properties.

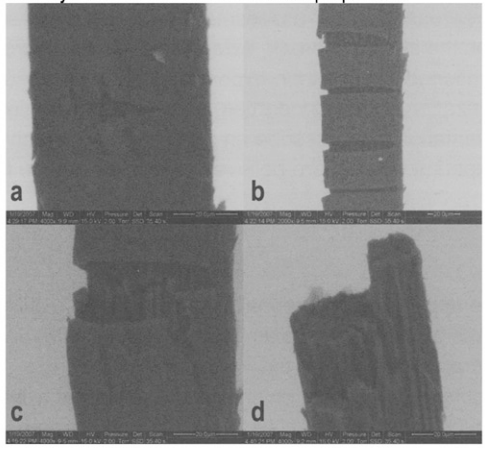

Figure 1. Process of breakage from ESEM Images. (a) Appearance of cracks at the hair surface; (b) extension of the crack perpendicularly to the fiber axis; (c) propagation of the crack in the longitudinal direction of the fiber axis with apparition of cracks on the cortex cells; (d) a step-wise fracture of the complete breakage process.

We have also investigated the effects of temperature and application of a relaxer solution on hair using ESEM to mimic heat from consumer appliances and straightening products, which may contribute to breakage. The initial experiments were carried out to observe the morphological changes of an African-American hair fiber with increased temperature under mechanical stress. During the heating process, formation of bubbles, melting of the cuticle, and isolation of the cuticle from the cortex occurred, suggesting a mechanical weakness between the two structures. In addition, we have also examined the effects of a relaxer droplet on African-American hair during a 30-minute exposure. After relaxer exposure and water rinsing, morphological changes were observed at and near relaxer exposure on the same single fiber, which may contribute to modifications in hair that contribute to loss of fiber integrity.

In order to address the needs of the African-American consumer, hair samples were treated with common anti-breakage molecules and the mechanical properties were examined using MTT to investigate differences in premature failure and fiber strength. An increase in strength and decrease in premature failure was observed for fibers treated with the anti-breakage molecules. Future experiments will be performed to correlate mechanical data to consumer perception.

References

1. This work was supported in part by the US DOE Office of Science, Contract DE-AC02-06CH11357 at ANL

QUANTIFYING DIFFERENCES IN THE PROPENSITY FOR BREAKAGE IN AFRO AND CAUCASIAN HAIR

Trefor Evans, Ph.D.

TRI/Princeton, 601 Prospect Avenue, Princeton, NJ 08540

Introduction

The generation of stress-strain curves is commonly used to assess the strength of individual hair fibers. However, while these measures provide a means for characterizing the technical strength of hair, it can be argued that such experiments are not a particularly accurate simulation of how consumers make judgment. Instead, it appears likely that consumer assessment of hair strength comes from viewing the number of broken fibers in a brush or comb after grooming; by noting the number of fibers at the bottom of the tub after showering; or by observing split ends in a mirror. In fact, in the consumer vernacular, it seems likely that "strength" represents a self-assessment involving the ease of hair breakage. While technical parameters such as the stress-to-break, extension-to-break and/or work-to-break are commonly extracted from the afore-mentioned stress-strain experiments; again it is suggested that these variables provide a scientific characterization of fiber properties, rather than a simulation of consumer-relevant stimuli. The goal of this presentation is to describe an alternative approach for investigating hair breakage, which involves experiments that are believed to better simulate the wear and tear from everyday grooming.

Methodology

Experimentation involves the application of a repeated force, with an evaluation of the number of cycles required for failure – a process often referred to as "fatigue testing". The underlying principle behind this approach relates to repeated application of an external stimulus leaving a sample in a weakened state - where, ultimately, failure occurs upon application of a force considerably less than that required to induce breakage from a single stimulus application. As such, testing is presumed to be more akin to the external stimuli received over a lifetime of grooming. Experiments are performed using the commercially-available Dia-stron CYC800 instrument. The basics of this approach have been outlined previously[1,2] in articles where the primary focus was to describe new commercial instrumentation. Here, the intention is to focus on performing this testing – including aspects such as experimental design, analysis of the resulting data, and implications of the findings.

Results:

Figure 1 shows breakage data in terms of cycles-to-break versus the applied stress – an approach often termed an S-N Plot. As possibly anticipated, repeated application of higher stresses results in fewer cycles before failure. However, from Figure 1 it is observed that the relationship between these two parameters is exponential in nature. As such, one observes how a reduction in the fatiguing stress (i.e. grooming forces) – as will occur upon using lubricious conditioning products – can have a hugely beneficial influence on the number of cycles to break.

The data from such experiments can be further mined by fitting a statistical distribution to the data via the Weibull approach[3]. Such an approach allows for the generation of Weibull parameters, that provide a means for characterizing the system; but, more interestingly, these parameters allow for a re-generation of the cumulative distribution that describes the data. This is often called a Probability Distribution curve and predicts the likelihood of a fiber surviving a given number of fatiguing cycles.

Figure 2 shows S-N Curves for both Caucasian and Afro hair obtained under the same experimental conditions. As possibly anticipated, the Afro hair shows a tendency to break after a lower number of cycles; but also shows considerably more experimental scatter.

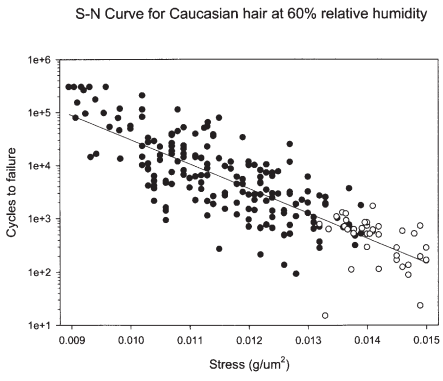

Figure 1

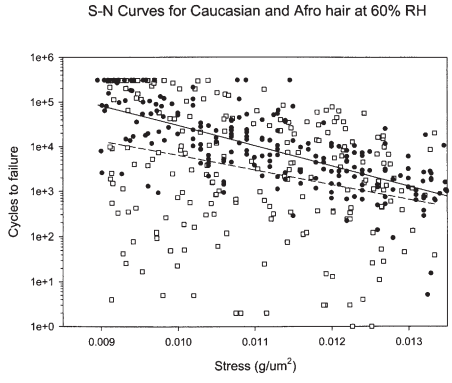

Figure 2

This scatter is accounted for in the Weibull analysis and the resulting Probability Distribution plots show Afro hair having a much high propensity for early failure – a conclusion that agrees well with known consumer experiences. It is well-recognized that the highly-fragile nature of Afro hair is such an issue that it demands very different habits and practices. This is a conclusion that would not seem to be reflected in a relatively meagre 13% reduction in break stress and break extension – as observed by conventional constant rate extension experiments.

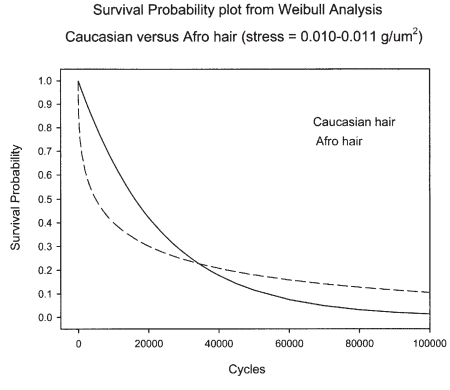

Figure 3

1) S.B.Hornby, Cyclic Testing: Demonstrating Conditioner Benefits on Damaged Hair, Cosmetics and Toiletries, 116, 35-39 (2001).

2) S.B.Hornby, N.J.P.Winsey and S.P.Bucknell, New Techniques to Capture Viscoelastic Changes in Hair Induced by Mechanical Stress, IFSCC Magazine, 5(2), 93-97 (2002).

3) W.Weibull, A statistical distribution function of wide applicability, J.Appl.Mech, 9, 293-297 (1951).